NASA TECHNICAL NOTE

NASA TN D-8035

NASA TN D-8035

SALTATION ON MARS AND EXPECTED LIFETIME OF VIKING 75 WIND SENSORS

Robert M. Henry

Langley Research Center
Hampton, Va. 23665

NATIONAL AERONAUTICS AND SPACE ADMINISTRATION • WASHINGTON, D. C. • DECEMBER 1975

SALTATION ON MARS AND EXPECTED LIFETIME OF VIKING 75 WIND SENSORS

Robert M. Henry
Langley Research Center

SUMMARY

With the use of the wind-tunnel measurements of Bagnold and Zingg, a model is developed for estimating the parameters that describe the flux of sand on Mars. Application of this model to the sensor-breakage problem indicates that the expected lifetime on Mars of the wind sensors of the Viking 75 Meteorology Instrument System is about 40 Earth years for the worst case considered; this expected lifetime is adequate for both the primary Viking 75 mission and for a proposed extended mission of one Martian annual cycle.

INTRODUCTION

The Viking 75 Meteorology Instrumentation System contains three "hot-film" sensors; each sensor is about 0.5 mm in diameter and 1 cm in length and is mounted as shown in figure 1. The sensors are made of borosilicate glass coated with a platinum film 0.5 μm thick and overcoated with 5 μm of aluminum oxide. Two of these sensors are used to measure two components of wind velocity; the third serves as a reference temperature sensor for the wind measurement. These sensors are deployed from the Viking lander on a nonadjustable boom. Variation of lander tilt within its nominal range results in a sensor-height range above the Martian surface of 1.2 to 1.6 m. While deployed, the sensors are exposed to impact and possible breakage by windblown Martian sand. Environmental criteria of the Mars Engineering Model have been developed for the exposure of the Viking lander to windblown sand and dust. However, these criteria were developed primarily for use in designing the protection of lander components from surface erosion, and may not be appropriate for evaluation of the likelihood of sensor breakage.

The purpose of this paper is to develop and to apply criteria suitable for the evaluation of the expected lifetime of the hot-film sensors in the Viking Meteorology Instrument System while the sensors are exposed to saltating (blowing) sand after landing on the planet Mars. It is the intent of this report to develop realistic rather than ultraconservative values. However, the uncertainties involved both in the understanding of the saltation process and in the estimation of Mars parameters require the use of conservative assumptions and values in several cases. Therefore, the estimated lifetime is a conservative value,

although a much less conservative one than the erosion criteria for the Mars engineering model. The order of the development is: first, criteria for sensor breakage by sand-grain impact are developed; second, a saltation model is developed to permit calculation of values of parameters needed in the failure criteria; and third, quantitative values for a range of expected Martian conditions are applied to determine the expected sensor life.

SYMBOLS

C	nondimensional constant in flux equation
C_D	sphere drag coefficient
C_Z	empirical constant in equation (6)
D	standard diameter in flux equation (250 μm)
d	diameter of sand particle
E_k	kinetic energy (KE on computer printout)
F	slip factor
g	acceleration due to gravity
H	scale height = $-\left(\frac{\partial \ln Q}{\partial z}\right)^{-1}$
h	mean height of saltation
k'	height where slope of logarithmic wind profile changes (Bagnold's "focus")
k_o	von Kármán's constant (taken as 0.4)
Q	mass flux per unit area
q	mass flux per unit length
R	Reynolds number
V	wind speed

V_t	threshold wind speed at height k'
V_*	friction velocity $\sqrt{\tau_o/\rho}$
V_*'	equivalent friction velocity during saltation
$V_{*,t}$	threshold friction velocity for saltation
w_o	initial vertical velocity or specific impulse
z	height above planetary surface (Z on computer printout)
z_o	roughness length in equations (9) to (11)
z_{max}	apex height of trajectory
λ	molecular mean free path
μ	coefficient of viscosity
ρ	atmospheric density
σ	particle density
τ_o	surface shear stress

Subscripts:

M	Mars
E	Earth

FAILURE CRITERIA FOR WIND SENSORS

Tests conducted for the Viking 75 project by Wendel J. Maegley of Martin Marietta Aerospace[1] have established at least partial criteria for breakage of the Viking wind sensors by impacting particles. Because sufficient flight-type sensors were not available

[1]W. J. Maegley: Effect of Wind Borne Particles on the Survival of the VMIS Wind Sensors. Martin Marietta Aerospace Memorandum 8943-73-14, Jan. 19, 1973. (Not generally available.)

only one actual flight-type sensor was tested. A few early prototypes of the flight sensor were used; the largest number of test subjects were uncoated borosilicate glass rods of the type used in the flight sensor. The number of tests with each test subject is shown in table I.

The test procedure involved blowing variously sized screened basalt particles through a tube onto the test specimens. Films of the test were used to determine particle velocities and number of impacts. For most of the tests the particle-flux rates were a few orders of magnitude higher than the particle-flux rates predicted herein for saltation on Mars. However, for the single flight-type sensor the particle flux was many orders of magnitude higher.

The results of Maegley's tests are shown in figure 2 and in table I. The diagonal line in figure 2 between breakage and no-breakage corresponds to a particle kinetic energy of 15 μJ. Particles with less than 15 μJ kinetic energy did not break the test subjects even after very long exposures (>100 000 impacts). Thus, it appears that the particle kinetic energy constitutes a suitable criterion for the combination of particle mass and velocity required to break the sensor. The value of 15 μJ is adopted as the minimum kinetic energy for breakage.

The number of impacts of particles with a kinetic energy of 15 μJ or higher required to break the sensor is a much more uncertain figure. As shown in table I, from 25 to 24 000 impacts at or above the given energy level were required to break the various test subjects. Compared to the uncoated rods, the coated prototype sensors required a much larger number of impacts before fracture, although the kinetic energy per particle was, at most, only slightly larger. In both cases the failures appeared to be progressive, with a number of microscopic pits or chips appearing before the sensor actually failed. The data in table I show that, even though there was a very wide range in the number of impacts required for breakage, the number required for each of the test conditions where more than one test subject was used had a surprisingly small range of number of impacts. This finding also suggests a progressive failure mechanism with failure occurring only after a more or less fixed number of impacts.

The flight-type sensor had a much thinner but much smoother aluminum oxide overcoating than the prototype sensors, so the sensors might be either stronger or weaker. In the case of the flight-type sensor, which was subjected to a much higher rate of flux, extensive damage was not noted before breakage; the actual break occurred when two impacts came in rapid succession. Furthermore, motion pictures showed that the break occurred at a point on the sensor well out from the point of impact. These circumstances suggest the possibility of a resonance effect resulting from the two impacts in rapid succession. As can be seen in the "Results and Discussion" section, the probability of such rapid impacts on Mars would be extremely small. Since the failure of the flight-type

sensor probably occurred at an anomalously low number of impacts (1100), this number offers a conservative, perhaps a very conservative, breakage criterion. Thus, for the purpose of the present study, a value of 1000 impacts is adopted for the number of 15 μJ impacts required to fracture a sensor.

The data for a mean particle diameter of 1200 μm show that at the higher kinetic energy of 43 μJ, the number of impacts required to break the test subject was consistently lower than the number required where the kinetic energy was in the range of about 15 μJ to 25 μJ. Since the number required at the 43-μJ level was about an order of magnitude less than for similar test subjects at the lower energy values, a criterion of 100 rather than 1000 impacts is adopted for a kinetic energy of 45 μJ.

For particles with a kinetic energy much above that in the tests, the required number of impacts would be expected to be much smaller. For some still larger value of kinetic energy the sensors would break on the first impact.

In order to account for the effect of possible impacts with kinetic energy greater than the test values, the two points (15 μJ, 1000 impacts and 45 μJ, 100 impacts) are connected with an exponential curve, giving the number of impacts to breakage as

$$1000 \times 10^{-\left[\frac{E_k(\mu J)-15}{30}\right]}$$

An exponential curve is used because a straight line would predict breakage at zero impacts with a kinetic energy of only 48 μJ, a prediction which is clearly unrealistic; the other simple curve which might be used (a power law) would be less conservative than the exponential curve. (In the calculations presented in "Results and Discussion" for Martian conditions, the critical kinetic-energy values are very near the experimental data points, so that the precise shape of the curve is not crucial in this particular application.)

In actual exposure each particle size has a different value of kinetic energy; a criterion which varies with kinetic energy is not convenient to use. Instead, an effective number of impacts is defined equal to the actual number multiplied by

$$10^{\left[\frac{E_k(\mu J)-15}{30}\right]}$$

and a single criterion of 1000 effective impacts is used.

Very high particle velocities are required for sensor breakage by small particles while larger particles can break the sensors at much smaller velocities. (See fig. 2.) This finding suggests that the larger particles may be of great importance in the sensor-breakage problem. However, in the erosion criteria for the Mars engineering model, the larger particles are of minimal importance compared to particles in the 100- to 200-μm range.

SALTATION MODEL

Particles larger than about 50 μm fall rapidly enough in the atmospheres of both Earth and Mars so that they cannot be considered fully suspended particles. In high winds, particles whose diameter is below about 1000 μm move by a series of jumps in a process called saltation. The saltation process has been studied by investigators with a wide variety of interests, and semiempirical laws have been formulated to describe some aspects of the saltation process. Such laws have dealt most notably with threshold velocities required to initiate or to maintain the saltation process and with the total (height-integrated) flux of material across a unit width. However, little information is available regarding the variations of particle concentration or flux with height, and no information has been found regarding the variation of particle velocities with particle size and height above the surface. Nevertheless, the latter quantities must be specified in order to determine the effect of the saltating particles on exposed components of the landed spacecraft.

In this section methods of specifying the necessary quantities are described. For parameters other than the variations with height of particle size, velocity, and flux, the methods and assumptions used in the present study are the same as those used in formulating the blowing-sand environmental criteria in the Viking Mars Engineering Model, M-75-125-3, Revision A.

Integrated Mass Flux

A number of measurements have been made of the height-integrated mass flux q where

$$q = \int_0^\infty Q \, dz \tag{1}$$

and Q is the mass flux at height z. Bagnold (ref. 1) suggests the form

$$q = C\left(\frac{d}{D}\right)^{1/2} \frac{\rho}{g}\left(V_*'\right)^3 \tag{2}$$

where C is an empirical coefficient which depends on the degree of uniformity of grain diameter in the sand and D is the predominant diameter of the sand. This equation has been found to fit not only Bagnold's experimental data but also that of subsequent investigators quite well. Zingg (ref. 2) found slightly lower values of C and a three-fourths rather than a one-half power dependence on diameter. The latter difference is of little importance for sand whose predominant diameter is near the standard diameter D of 250 μm.

For the diameter distribution of dune sand given in the Viking Mars Engineering Model, with a predominant diameter of about 300 μm, a C of 1.8 corresponding to naturally graded dune sand, a g of 3.7 m/s^2, a ρ of 1.2×10^{-2} kg/m^3, and a V_*' corresponding to a wind speed of 40 m/s at a height of 1 m, equation (1) yields a value of $q = 0.1$ kg/m-s, the value adopted for the Mars Engineering Model. Values used in the present study vary with the assumed Mars conditions, but are close to the above value of q.

Mass-Flux Variation With Height

Relatively few measurements have been made of the variation with height of mass flux (through a unit area), but Bagnold (ref. 1) presents the variation with height for dune sand. Zingg (ref. 2) gives the variation with height for several narrow ranges of sand diameter. In both cases the variations are roughly exponential with height.

The variation of mass flux with height is assumed to be described by

$$Q = \frac{q}{H} \exp\left(-\frac{z}{H}\right) \tag{3}$$

As required by equation (1) the integral of Q is equal to q. The parameter H determines the logarithmic rate of decrease of Q with height, and by analogy with atmospheric pressure and density scale heights it is called the mass-flux scale height, or simply scale height. Setting the partial derivative of Q with respect to H in equation (2) equal to zero shows that the maximum flux at a given height z occurs when $H = z$.

For the Mars Engineering Model, the mass flux (0.2 exp -2z kg/m^2-s) was specified such that it produced the largest mass flux in the height region between 0.5 m and 2 m where the equipment is mounted on the lander body. The value in the Mars Engineering Model is the same as the value given by equation (3) with $H = z = 0.5$ m.

Values of the mass flux at $z = 0.5$ m with $q = 0.1$ kg/m-s resulting from given values of H are shown in figure 3. Specifying a value of H larger than 0.5 results in a smaller value of Q; a smaller value of H yields a much smaller value of Q.

At heights above 0.5 m, setting the value of H equal to 0.5 m gives mass fluxes somewhat lower than the maximum mass fluxes. However, as shown in figures 4 and 5, at $z = 1.2$ m and $z = 1.6$ m (the lowest and highest expected heights of the wind sensors) the indicated values of flux are still much larger than would be given by smaller values of H such as are derived in later sections. Hence, the indicated values of flux may be overconservative.

The scale height H can be related to the "average height of saltation" h (called y_a in Zingg's notation) as measured by Zingg (ref. 2). Since by definition half of the flux takes place above and half below h, then

$$\int_0^h \frac{q}{H} \exp\left(-\frac{z}{H}\right) dz = \int_h^\infty \frac{q}{H} \exp\left(-\frac{z}{H}\right) dz = \frac{1}{2} q \tag{4}$$

so that

$$H = \frac{1}{\ln 2} h = 1.44h \tag{5}$$

Zingg (ref. 2) made wind-tunnel measurements of h for various particle sizes and wind velocities under Earth surface conditions of gravity and atmospheric density. The results are shown in figure 6. Zingg found that his data could be fitted by an equation of the form

$$h = C_Z d^{3/2} \rho^{1/4} V_{*,t}^{1/2} \tag{6}$$

where the value of C_Z is 2350 $kg^{-1/4} m^{-1/4} s^{1/2}$.

If a way can be found to relate the value of h on Mars to the value of h on Earth, equation (6) can be used to find the value of h, equation (5) can be used to find H, and equations (2) and (3) can be used to find the value of Q as a function of height on Mars. This value of Q can then be used with particle velocities derived by numerical trajectory simulation and a particle-size-distribution model to derive concentration, kinetic-energy flux, particle flux, rate of sensor impacts, and, finally, an estimate of the expected life of the sensors.

Relation of Saltation Scale Heights for Earth and Mars

The initial vertical particle velocity w_o is assumed herein to be caused by some combination of lift, drag, and/or kinetic energy from a previous "jump." All these quantities may be expected to be functions of the stagnation pressure $\frac{1}{2}\rho V^2$. Since V at any particular height is approximately proportional to V_*', it is reasonable to assume that

$$\frac{\sigma_M w_{o,M}^2}{\sigma_E w_{o,E}^2} = \frac{\rho_M V_{*,M}'^2}{\rho_E V_{*,E}'^2} \tag{7}$$

where σ is assumed equal for Earth and Mars.

For the same w_o, the scale height and the average saltation height on Mars and Earth are assumed proportional to the respective apex heights. Thus,

$$\frac{H_M}{H_E} = \frac{h_M}{h_E} = \frac{\left[z_{max}(w_o)\right]_M}{\left[z_{max}(w_o)\right]_E} \tag{8}$$

Particle-Size Distribution

Since the value of h and, therefore, of H for a given w_o is a function of particle size, the variation of mass flux with height is different for each particle size, and the mass flux at a given height must be found by combining the mass fluxes of particles of various diameters. Thus it is necessary to specify the size distribution of particles involved in the saltation processes. It is here assumed that all particles which contribute significantly to the composition of surface material are involved, so that the size distribution of particles in the surface material is used.

The distribution of particles by particle size was taken from the dune-sand model distribution of the Mars Engineering Model. The proportion for each 100-μm-diameter class is shown in table II. In forming this table intermediate particles were assigned to the even 100-μm-diameter class whose mass was nearest the mass of the intermediate particle. Particles with diameters smaller than 100 μm or larger than 1000 μm are not considered separately because of the rapid decrease of number density with particle diameter in the dune-sand distribution. However, all smaller particles are included in the 100-μm class and all larger particles in the 1000-μm class.

Trajectory Simulations

In order to determine particle velocities under Martian conditions, a series of numerical particle-trajectory simulations is performed. In the numerical trajectory simulation the sand-particle motion is calculated at constant acceleration over each small time step using the wind-velocity profile and the slip-corrected drag coefficient described herein. Then, using the new particle position and velocity at the end of the time step, a new wind speed at the new height and then a new drag force are calculated; the process is repeated for the next time step. The process is straightforward once all the necessary parameters are defined.

In these simulations the particle is started out at zero height with some assigned initial vertical velocity w_o. This initial vertical velocity can be thought of as representing the specific impulse of the particle imparted by some combination of impact dynamics and aerodynamic lift due to wind shear and/or particle rotation. In an actual particle trajectory, the lift might be distributed over some finite vertical height. However, because of the concentration of wind shear in the very lowest levels, the effects of lift can be approximated by an instantaneously acquired velocity. Aerodynamic lift is not otherwise

included in the calculation; particle-particle collisions are not considered as such collisions would occur too rarely to play a significant role.

All particles are assumed to be spherical in shape and to have a density of 2650 kg/m^3. Sphere drag coefficients as a function of Reynolds number are calculated by a curve fit taken from Morsi and Alexander (ref. 3). This curve fit utilizes a series of quadratics in (1/R). The resulting curve for C_D as a function of R is shown in figure 7.

The particle diameters involved are not sufficiently large compared to the Martian atmospheric mean free path (about 10 μm) to insure continuum flow. Therefore, a slip-flow correction taken from Davies (ref. 4) has been applied to the drag coefficient. The slip factor $F = 1 + \frac{\lambda}{d}\left[2.514 + 0.8 \exp(-0.55d/\lambda)\right]$ was designed as a multiplicative correction factor applied to the Stokes'-law velocity. Because the present range of Reynolds numbers extends beyond the region of applicability of Stokes' law, the correction is applied instead to the drag coefficient C_D described therein. Thus,

$$C_D(\text{slip}) = \frac{C_D(\text{continuum})}{F}$$

The slip correction ranges from about 3 percent for 1000-μm particles to about 30 percent for 100-μm particles.

Wind-velocity profile.- When the atmospheric stability is near neutral, the vertical profile of the wind speed in the boundary layer can be approximated by a logarithmic profile of the form

$$V(z) = \frac{V_*}{k_o} \ln \frac{z}{z_o} \tag{9}$$

Once saltation is fully developed the atmosphere is well mixed and the atmospheric stability is near neutral. However, the wind profile is modified by interaction with the saltating particles. Bagnold (ref. 1) and Zingg (ref. 2) found that the modified profile could be approximated by a combination of two logarithmic profiles: the wind speed up to height $z = k'$ is given by

$$V(z) = \frac{V_{*,t}}{k_o} \ln \frac{z}{z_o} \tag{10}$$

and the profile from $z = k'$ to the top of the boundary layer (which is always above the top of the lander) is given by

$$V(z) = \frac{V_*'}{k_o} \ln \frac{z}{k'} + V_t \tag{11}$$

where

$$V_t = V(k') = \frac{V_{*,t}}{k_o} \ln \frac{k'}{z_o} \tag{12}$$

(The velocity $V(z)$ is assumed to be zero for $z < z_o$.) For Earth conditions, Bagnold found k' to be about 3 mm and Zingg found k' to vary with particle diameter and to be equal to 10d (for an assumed mean diameter of Martian sand of 300 μm, Zingg's relationship also gives $k' = 3$ mm). In view of the lower gravity (3.7 m/s^2) and possible greater saltation height of Mars, calculations have also been made using $k' = 1$ cm. Values used for the roughness parameter z_o are 300 μm corresponding to observed values for Earth's deserts and 30 μm corresponding to smooth sand.

Atmospheric parameters.- The values required for the calculations are the density and coefficient of viscosity. Atmospheric density enters into the calculations in several ways: it appears directly in the horizontal- and vertical-acceleration terms; it enters the drag coefficient through the Reynolds number; and it enters the slip-flow correction through the mean free path. Viscosity enters only through the Reynolds number.

Representative Particle Trajectory

If the probability-density function of w_o for each particle diameter were known, particle velocities (and, indeed, all the variables of interest) could be determined by straightforward Monte Carlo simulation. Lacking knowledge of this function a single representative trajectory for a class of particles may be established (i.e., the class of particles of a particular size at a particular height).

In the present model most of the particles at a given height are particles which have apex heights at or slightly above the given height. Particles which have apex heights below the given height cannot, of course, collide with a sensor at that height. With an exponential decrease of mass flux with height, the mass flux decreases rapidly with height. With increasing particle velocity with height, the number of particles at a given height decreases even more rapidly than does the mass flux. In "Results and Discussion" computed scale heights indicate that the decrease is very rapid on Mars. In addition, since the vertical velocity of the particle is very low near the apex height, the probability that a particle would be at some height below its apex height, and thus could strike a sensor at the lower height, decreases rapidly with decreasing height. For example, the calculated probability density-per-unit height for a 300-μm particle with a 2-m apex is shown in figure 8. The decrease with decreasing height in the region just below the apex height is very rapid.

Because of the combination of the rapid decrease with height of the number of particles which reach levels above the sensor height, and because of the very rapid decrease in the probability that one of these particles might strike the sensors, particles with apex

heights equal to the sensor height are considered to be representative of particles which strike the sensors. The velocity of such particles is used in subsequent flux calculations.

Values of particle velocity for various particle sizes and apex heights are determined by the mathematical simulation described in the section on "Trajectory Simulations." The w_o values are selected to produce the desired apex height. The resulting particle velocities are shown in table III, and the corresponding particle kinetic energy is shown in table IV. The kinetic energy of the smaller particles is less than the 15 μJ which Maegley found was required for sensor breakage.

The kinetic energy of the small particles is below that required for sensor breakage. This fact is important in the use of the present model for two reasons. First, the simulations by Zingg in a wind tunnel with a 91-cm (3-ft) square test section may not have adequately simulated the effects of larger-scale atmospheric turbulence on the smaller particles which may be in partial suspension. Sharp (ref. 5) presents data on the "height at which each grain-size fraction attains its maximum weight percentage" for measurements made in the atmosphere of Earth. These data show values of this "height" for particle-size ranges of <62 μm and of 62 μm to 125 μm to be larger than the values for larger particle-size ranges. For diameters larger than 125 μm the values increase monotonically with increasing diameter in general agreement with Zingg's wind-tunnel data. Since fall velocities are about the same on Earth and Mars for particles between 10 and 1000 μm, similar behavior might be expected on Mars. Second, on Mars there may be a much larger percentage of very small particles than the percentage in the dune-sand model distribution of particle sizes, since the major small-particle sinks of Earth (e.g., oceans) are not found on Mars. If either of these conditions should exist, and if these small particles were to possess sufficient kinetic energy to break the sensors, then the present model could be unconservative for use in sensor-breakage studies. Since the small particles do not possess sufficient kinetic energy, the model is not unconservative for the present use.

Because of these two reservations concerning its applicability to small particles, it is not recommended that this new model be used to reevaluate the Mars Engineering Model criteria for erosion, since erosion was found to be produced largely by particles of the smaller sizes. However, the new model is considered to be applicable to the problem of sensor breakage where the smaller particles play no part.

Threshold Velocity

In the calculations described above it is assumed that the friction wind velocity V_* is sufficiently large that saltation occurs for all of the particles in the size range from 100 μm to 1000 μm. Various assessments of the threshold velocity or threshold friction velocity on Mars have been made (e.g., in the Viking Mars Engineering Model and in

refs. 6, 7, and 8). In figure III-A-23 of the Viking Mars Engineering Model there is an indication that a wind of 40 m/s at a height of 1 m would be below the threshold value for all particles if z_0 were 30 μm. In figure III-A-24 there is an indication that 40 m/s would be below the threshold velocity for particles larger than 600 μm in the mean model or 900 μm in the Max ρ_S model atmosphere, even if z_0 were as large as 1 mm. However, these threshold values were calculated for "mean-surface-level" conditions (i.e., the mean equatorial radius of the planet). If threshold values are recalculated by the method used in the Mars Engineering Model for the mean atmosphere 4.5 km below the mean equatorial surface (representative of the proposed Viking 75 A prime and backup site and the Viking B prime site) and a value of 300 μm for z_0, it is found that 40 m/s at 1 m equals or exceeds the threshold velocity for particles of a 1000-μm or less diameter.

The threshold-velocity values herein may be open to question. All of the values were based on data published in 1941 by Bagnold (ref. 1). More recent data by Chepil (ref. 9) in 1958 indicate lower values; the most recent data by Iversen, Greeley, Pollack, and White (ref. 10) in 1973 indicate higher values than those of Bagnold. Also, the effects of aerodynamic lift and the effects of cohesion of surface material were not considered in the derivation of any of these values. The most likely effect of these latter considerations would be a reduction of the threshold velocities for Mars. Thus, the assumption which is made here that all particles up to 1000 μm in diameter are involved in the saltation process is rather uncertain, but appears to be reasonable. Certainly it would be unconservative to assume that the larger particles were not involved.

Computations

Once the necessary input parameters are specified, the determination of apex height z_{max} as a function of w_0 for the assumed conditions on either Mars or Earth is a straightforward iterative process. Similarly, once particle velocities and scale height are also specified, the computation of mass flux kinetic energy, particle flux, the number of impacts for each particle class, the "effective" number of impacts, and sensor life is a straightforward process. However, since the exponential form of equation (3) is only an approximation of the actual variation of mass flux with height, the value of mass flux at a particular height depends on the way in which the fitting of the exponential is performed. In particular, the mass-flux value depends on the choice of z_{max} for either Mars or Earth used in applying equations (7) and (8). Larger values of z_{max} for either planet produce larger values of h_M/h_E and larger values of mass flux on Mars in the region between 0.5 m and 2 m. The procedure adopted in the present report is:

1. For each particle size and for each height z for which fluxes are to be computed for Mars, assume $z_{max,M}$ equal to z.

2. From trajectory simulations find $w_{o,M}$ corresponding to $z_{max,M}$.

3. From equation (7) find $w_{o,E}$ corresponding to $w_{o,M}$.

4. From trajectory simulations find $z_{max,E}$ corresponding to the $w_{o,E}$ from step 3.

5. From equation (6) find h_E.

6. From equation (8) and h_E, $z_{max,M}$, and $z_{max,E}$ from the previous steps, find h_M.

7. From equation (6) find H_M. (In calculations for sensitivity testing, the first seven steps are performed for only a single Mars height.)

8. Using equations (2) and (3) find the value of mass flux Q for each height. This value is the equivalent mass flux for sand of a uniform size, and must be multiplied by the proportion of sand in each size class to find the mass flux of that size class for a sand with a wide range of particle size. From this point, the remaining flux calculations are straightforward.

Sensitivity to Input Parameters

The sensitivity of velocities computed in the trajectory simulations was tested by independently varying several of the input parameters over a range of values while holding the other parameter values constant at typical values. The ranges of parameters tested are:

z_o = 30 μm to 300 μm

k' = 3 mm to 1 cm

$\rho = 1.22 \times 10^{-2}$ kg/m^3 to 1.8×10^{-2} kg/m^3

$\mu = 1.6 \times 10^{-5}$ to 10^{-4} kg/m^2-s

$V_{*,t}$ = 0.45 m/s to 2.5 m/s

Except for the density change none of these parameters produced changes in the calculated particle velocity greater than 1 m/s, or greater than about 3 percent of the velocity at heights above 0.5 m. The 50-percent change in density produced particle-velocity changes of up to 2 m/s, or up to 18 percent.

The z_o value of 30 μm corresponds to a smooth surface of sand with a predominant size of 300 μm; z_o of 300 μm corresponds to measurements (not during saltation) of actual Earth desert surfaces. Measurements in wind tunnels during saltation are near the lower value. Values of $z_o > 300$ μm may occur on Mars if material other than the modeled sand is present. However, Chepil (ref. 11) and Iversen, Greeley, Pollack, and

White (ref. 10) show that the threshold velocity increases rapidly with increasing values of z_0; thus, it is unlikely that the larger sand particles would saltate.

For Earth conditions Bagnold found k' to be about 3 mm. Zingg found k' to vary with particle diameter and to be equal to 10d (for an assumed mean diameter of Martian sand of 300 μm Zingg's relationship also gives $k' = 3$ mm). In view of the lower gravity (3.7 m/s^2) and possible greater saltation height of Mars, an additional value $k' = 1$ cm was used as a conservative value.

The lower value of atmospheric density is the density at the mean equatorial surface, The higher density corresponds to an elevation 4.5 km below the mean equatorial surface at the prime and backup sites for the Viking 75 A mission, and the prime site for the B mission. Other possible landing sites are at higher elevations

The viscosity values represent an arbitrary ±20-percent range about the estimated value of 1.8×10^{-5} kg/m-s^2.

Although the variation of particle velocity is small over the ranges of input parameters considered herein, variation of mass flux may be substantial. Equation (2) indicates that height-integrated mass flux varies directly with ρ and as the cube of V_*'; however, there are also indirect effects resulting from changes in H in equation (3) so that the total effects are best shown by a complete calculation as described herein.

Combined Variation

In order to illustrate the range of variation of particle velocity and mass flux, computations were made for both a "smooth" case and for a "rough" case. Parameters used for the two Mars cases, and for the single Earth case (used with both Mars cases) are given in table V. A 1-m wind speed of 40 m/s for Earth would result in values outside the range of values used in the formation of the empirical equations of Bagnold and Zingg. The Earth case is chosen to give values well within the ranges of experimental values of both Bagnold and Zingg. In the Mars cases parameters were chosen from the ranges previously used to give, in the smooth case, the highest wind speeds below 1 m and, in the rough case, to give the largest value of V_*'. In both cases a fixed 1-m wind speed of 40 m/s was employed. Velocities for the rough case are given in table III. Ratios of particle velocities for the two cases are given in table VI. The largest differences in particle velocities at heights where the kinetic energy is sufficient for sensor breakage (0.8 m and above) are about 5 percent compared with about 3 percent for variation of individual parameters. In table VII velocity ratios for the high-density and low-density rough cases are shown. Differences of up to 18 percent appear.

To assess the effects of scale heights, mass-flux computations were performed for two different ratios of Mars scale height to Earth scale height for each case. For each case the total mass flux (for all particle sizes) was computed with the ratio of scale heights

for each particle size held constant with height, rather than varying with height as described in the "Computations" section. The two ratios were those computed for Mars heights of 0.1 and 1.6 m. The four resulting plots of mass flux plotted against height are shown in figure 9. Not only are the differences between the smooth and rough cases very large, but even larger differences are found between values computed using scale-height ratios determined for Mars heights of 0.1 and 1.6 m.

In figure 10 computed mass-flux profiles are shown for the same wind-profile parameters for density values of 0.12 kg/m^3 and 0.18 kg/m^3. Both of these mass-flux profiles represent the rough case described above and scale-height ratios computed using a Mars height of 1.6 m. As might be expected the calculated mass flux is smaller in the lower-density atmosphere. Although the variation here is smaller than that produced by changes in the wind-profile parameters, there are still order-of-magnitude changes in the mass flux at the larger heights.

The particle-velocity calculations varied only a few percent over the range of Mars parameters considered. In contrast, the mass-flux model is quite sensitive to changes in the Mars parameters assumed.

RESULTS AND DISCUSSION

Because of the sensitivity of the mass-flux model to the variation of assumed Mars parameters, it would be difficult and perhaps meaningless to select a single average or typical set of Mars parameters for sensor expected-life calculations. Instead, attention is focused on the worst reasonably likely conditions, namely, the rough case with the higher-density value described herein. However, rather than using the scale-height ratios computed for 1.6 m (which produced the larger mass flux in the sensitivity tests), separate scale-height ratio values are computed for each Mars height as well as for each particle-size class, since this procedure gives the flux profile with the best fit at that particular height.

Various flux values calculated by the methods described herein are presented in tables VIII, IX, and X for heights of 0.8, 1.2, and 1.6 m, respectively. In these tables P is the percentage of particles of a given size class in the assumed surface material and equivalent mass flux is the total mass flux which would exist if all the particles were of the given size class; the mass flux of that size class is, then, the product of the equivalent mass flux and the percent P of particles of that size class. The mass flux is also equal to the product of the percent mass flux and the total mass flux. Similar relations hold for kinetic-energy flux, particle flux, and concentration. The number of hits per day for each particle size includes all the particles; the total number of hits per day and of effective hits per day is calculated only for particles which exceed the critical value of

15 μJ. ("Hits per day" refers to the number of hits in a total period, not necessarily continuous, of 24 hours of saltation.)

At 0.8 m, particles smaller than 700 μm do not attain the critical energy value of 15 μJ. At 1.2 and 1.6 m, particles smaller than 400 μm do not reach 15 μJ. Thus, as suggested earlier, possible deficiencies in modeling the scale heights of particles smaller than about 125 μm do not affect the validity of the model for the sensor-breakage study. The dominance of the large particles at the greater heights is clearly apparent in the percentage figures.

The highest value of kinetic energy at 0.8 m (17 μJ) is only slightly in excess of the critical value of 15 μJ, below which no breakage occurred; this value is also within the range where test subjects survived thousands of impacts. The highest value at 1.6 m (43 μJ) is triple the minimum value for breakage. This value coincides with 43 μJ of the 1200-μm particles in the test series.

It is also of interest, for example, to examine the characteristics of the complete flux profiles resulting from the combination of the profiles for individual particle sizes in order to determine whether this combination profile agrees with the assumption of an exponential variation of mass flux with height. Profiles of mass flux, concentration, and kinetic-energy flux are shown in figures 11, 12, and 13. The linear combination of individual exponential mass-flux profiles with scale heights which are not constant with height could not be expected to produce an exactly exponential variation with height. However, the validity of the model used depends on the assumption that an exponential function is a good approximation to the variation of mass flux with height. The mass-flux variation in figure 11 is a reasonable approximation to an exponential (which would appear as a straight line on this semilog plot), especially at the greater heights, although not as good an approximation as the curves in figures 9 and 10 where the scale height for each particle size was held constant over the height range.

The concentration of sand (the mass of sand per unit volume of space) shown in figure 12 and the kinetic-energy flux shown in figure 13 both exhibit roughly exponential variation and show the dominance of the mass-flux variation over the particle-velocity variation.

Table XI summarizes the application of the flux model to the problem of breakage of the hot-film wind sensors of the Meteorology Instrumentation System of the Viking 75 Mars Lander. These data apply to the rough, high-density case. Expected sensor lifetimes for the smooth and low-density cases (not shown) are measured in thousands of years. The most critical level is 0.8 m, the lowest height at which the critical value of 15 μJ occurs. Here the model yields a rate of 0.8 particle impacts per 24 hours of saltation with a 1-m wind of 40 m/s. Based on the assumption of a total of 7 days (from the Mars Engineering Model) of saltation per 90 mission days, and of a minimum of 1000

effective impacts required for breakage, the expected lifetime of a sensor is 40 Earth years (≈20 Martian years). This time period appears to be sufficient to assure a remote possibility of breakage, during either the 60-day primary mission or the proposed extended mission of one Martian year. The likelihood of breakage may be greater during an extended mission than during the primary mission since landings are scheduled during the season when minimum winds are expected at the landing sites; however, the assumption of a total of 7 days of saltation during 90 mission days is considered to be sufficiently conservative to include year-round occurrences.

At levels below 0.8 meter the number of impacts increases. However, the kinetic energy drops below the critical value of 15 μJ and the present model does not predict breakage at these levels.

At higher levels the number of impacts decreases rapidly while the kinetic energy increases. At the highest expected sensor level (1.6 m) the kinetic energy reaches the highest value encountered in the test data. Thus, values for greater heights are based on extrapolation of the test data but the continuation of the trend toward increasing expected lifetimes seems to be clear.

CONCLUDING REMARKS

A model for estimating the parameters of the flux of sand on Mars has been developed using the wind-tunnel measurements of Bagnold and Zingg. The model is not supported either by rigorous theoretical derivation or by experimental observations under realistic Martian conditions, but the assumptions involved appear to be both reasonable and conservative. Questions are raised concerning the validity of the model for particles which may be in partial suspension (<125 μm). These questions do not affect use of the model for studies of breakage of this wind sensor where such particles are shown to be ineffective. However, use of the model is restricted in material-erosion studies where such particles have been shown to be important.

Application of this model to the sensor-breakage problem indicates that the expected lifetime of the wind sensors is adequate both for the primary Viking 75 mission and for a proposed extended mission with a duration of one Martian year.

Langley Research Center
National Aeronautics and Space Administration
Hampton, Va. 23665
September 10, 1975

REFERENCES

1. Bagnold, R. A.: The Physics of Blown Sand and Desert Dunes. Methuen & Co., Ltd. (London), 1941.

2. Zingg, A. W.: Wind-Tunnel Studies of Movement of Sedimentary Material. Studies in Eng. Bull. no. 34, Iowa Univ., 1953, pp. 111-135.

3. Morsi, S. A.; and Alexander, A. J.: An Investigation of Particle Trajectories in Two-Phase Flow Systems. J. Fluid. Mech., vol. 55, pt. 2, Sept. 1972, pp. 193-208.

4. Davies, C. N.: Definitive Equations for the Fluid Resistance of Spheres. Proc. Phys. Soc., vol. 57, pt. 4, no. 322, July 1, 1945, pp. 259-270.

5. Sharp, Robert P.: Wind-Driven Sand in Coachella Valley, California. Geol. Soc. America Bull., vol. 75, no. 9, Sept. 1964, pp. 785-803.

6. Ryan, J. A.: Notes on the Martian Yellow Clouds. J. Geophys. Res., vol. 69, no. 18, Sept. 15, 1964, pp. 3759-3770.

7. Gifford, F. A., Jr.: A Study of Martian Yellow Clouds That Display Movement. Monthly Weather Rev., vol. 92, no. 10, Oct. 1964, pp. 435-440.

8. Wood, G. P.; Weaver, W. R.; and Henry, R. M.: The Minimum Free-Stream Wind Speed for Initiating Motion of Surface Material on Mars. NASA TM X-71959, 1974.

9. Chepil, W. S.: Soil Conditions That Influence Wind Erosion. Tech. Bull. No. 1185, U.S. Dep. Agriculture, June 1958.

10. Iversen, J. D.; Greeley, R.; Pollack, J. B.; and White, B. R.: Simulation of Martian Eolian Phenomena in the Atmospheric Wind Tunnel. Space Simulation, NASA SP-336, 1973, pp. 191-213.

11. Chepil, W. S.: Properties of Soil Which Influence Wind Erosion: IV.- State of Dry Aggregate Structure. Soil Sci., vol. 72, 1951, pp. 387-401.

TABLE I.- FRACTURE CONDITIONS OF TEST SAMPLES

Test sample	Particle diameter, μm		Particle velocity, m/s	Kinetic energy, μJ	Number tested	Number of collisions
	Range	Mean				
Uncoated glass rod	991 to 1397	1200	6	43	4	25 to 50
	417 to 495	450	14	13	4	250 to 350
	208 to 246	225	39	12	2	2000 to 3000
Prototype	246 to 351	300	28	15	1	20 000
	208 to 246	225	49	19	1	24 000
Flight type	417 to 495	450	17	18	1	[a]2100

[a]The first 1000 collisions occurred at the subcritical speed of 12 m/s (9 μJ).

TABLE II.- SIZE DISTRIBUTION

[Percentage by mass of particles with mass nearest to the mass of a particle of given diameter (corresponds to dune-sand distribution of the Viking Mars Engineering Model)]

Diameter, μm	Percentage
100	8
200	17
300	44
400	13
500	5
600	4
700	3
800	3
900	2
1000	1

TABLE III.- PARTICLE VELOCITY, m/s

[Computed using parameters for high-density rough case (table V)]

D= 100	200	300	400	500	600	700	800	900	1000	Z,M
18.0	9.2	5.3	3.7	2.8	2.1	1.7	1.4	1.2	1.0	0.10
22.1	13.4	9.1	6.4	4.7	3.7	3.0	2.4	2.1	1.8	0.20
26.3	17.4	11.6	8.5	6.4	5.0	4.1	3.3	2.8	2.4	0.30
28.8	19.8	13.9	10.2	7.7	6.1	5.0	4.1	3.5	3.0	0.40
30.9	22.1	15.7	11.7	9.0	7.1	5.8	4.8	4.1	3.5	0.50
32.4	23.8	17.2	13.0	10.0	8.0	6.6	5.5	4.7	4.0	0.60
33.8	25.3	18.7	14.2	11.0	8.8	7.3	6.1	5.2	4.5	0.70
34.9	26.8	19.9	15.3	11.9	9.6	7.9	6.7	5.7	4.9	0.80
35.9	27.9	21.0	16.2	12.8	10.3	8.5	7.2	6.2	5.4	0.90
36.7	29.0	22.1	17.2	13.6	11.0	9.1	7.7	6.6	5.8	1.00
37.5	30.0	23.0	18.1	14.3	11.6	9.7	8.2	7.0	6.1	1.10
38.2	30.8	23.9	18.8	15.0	12.2	10.2	8.6	7.5	6.5	1.20
38.9	31.6	24.7	19.6	15.7	12.8	10.7	9.1	7.8	6.9	1.30
39.5	32.4	25.4	20.3	16.3	13.3	11.2	9.5	8.2	7.2	1.40
40.0	33.1	26.2	20.9	16.9	13.9	11.6	9.9	8.6	7.5	1.50
40.5	33.7	26.9	21.6	17.5	14.4	12.1	10.3	8.9	7.8	1.60
41.0	34.4	27.5	22.2	18.0	14.9	12.5	10.7	9.3	8.1	1.70
41.5	34.9	28.1	22.8	18.6	15.3	12.9	11.1	9.6	8.4	1.80
41.9	35.5	28.7	23.3	19.0	15.8	13.3	11.4	9.9	8.7	1.90
42.3	36.0	29.2	23.8	19.5	16.2	13.7	11.8	10.2	9.0	2.00

TABLE IV.- PARTICLE KINETIC ENERGY, μJ

[Computed using parameters for high-density rough case (table V)]

D= 100	200	300	400	500	600	700	800	900	1000	Z,M
0	0	1	1	1	1	1	1	1	1	0.10
0	1	2	2	2	2	2	2	2	2	0.20
0	2	3	3	4	4	4	4	4	4	0.30
1	2	4	5	5	6	6	6	6	6	0.40
1	3	5	6	7	8	8	8	9	9	0.50
1	3	6	8	9	10	10	11	11	11	0.60
1	4	7	9	11	12	13	13	14	14	0.70
1	4	7	10	12	14	15	16	16	17	0.80
1	4	8	12	14	16	17	18	19	20	0.90
1	5	9	13	16	18	20	21	22	23	1.00
1	5	10	14	18	20	22	24	25	26	1.10
1	5	11	16	20	22	25	27	28	29	1.20
1	6	11	17	21	25	27	29	31	33	1.30
1	6	12	18	23	27	30	32	34	36	1.40
1	6	13	19	25	29	32	35	37	39	1.50
1	6	14	21	26	31	35	38	40	43	1.60
1	7	14	22	28	33	37	41	44	46	1.70
1	7	15	23	30	35	40	43	47	49	1.80
1	7	15	24	31	37	42	46	50	53	1.90
1	7	16	25	33	39	45	49	53	56	2.00

TABLE V.- PARAMETERS USED IN CALCULATIONS

	Mars high-density rough case	Mars low-density rough case	Mars high-density smooth case	Earth
ρ	0.018 kg/m^3	0.0122 kg/m^3	0.018 kg/m^3	1.225 kg/m^3
μ	1.1×10^{-5} kg/m-s	1.1×10^{-5} kg/m-s	1.1×10^{-5} kg/m-s	1.7894×10^{-5} kg/m-s
g	3.7 m/s^2	3.7 m/s^2	3.7 m/s^2	9.80665 m/s
z_o	300 μm	300 μm	30 μm	30 μm
k'	1 cm	1 cm	3 mm	3 mm
V at 1 m . . .	40 m/s	40 m/s	40 m/s	11 25 m/s
$V_{*,t}$	1.24 m/s	1.24 m/s	1.24 m/s	0.19 m/s
V_t	10.87 m/s	10.87 m/s	14.28 m/s	2.187 m/s
V_*'	2.53 m/s	2.53 m/s	1.771 m/s	0.624 m/s

TABLE VI.- VELOCITY RATIO

[Ratio of velocity for high-density rough case to velocity for high-density smooth case (table V)]

d = 100	200	300	400	500	600	700	800	900	1000	z,m
0.89	0.80	0.73	0.73	0.74	0.76	0.74	0.74	0.75	0.75	0.10
0.86	0.83	0.84	0 83	0.82	0.83	0.83	0.82	0.83	0.82	0.20
0.91	0.90	0.87	0.87	0.87	0.86	0.87	0.87	0.87	0.86	0.30
0.93	0.91	0.90	0.90	0.90	0 89	0.89	0.89	0.89	0.89	0.40
0.95	0.93	0.92	0.92	0.91	0.91	0.91	0.91	0.91	0.91	0.50
0.96	0.95	0.94	0.93	0.93	0.93	0.93	0.93	0.93	0.92	0.60
0.97	0.96	0 95	0.94	0.94	0.94	0.94	0.94	0.94	0.94	0.70
0.98	0.97	0.96	0.96	0.95	0 95	0.95	0.95	0.95	0.95	0.80
0.99	0 97	0.97	0.96	0.96	0.96	0.96	0.96	0.96	0.96	0.90
0.99	0.98	0.98	0.97	0.97	0.97	0.97	0.97	0.97	0.97	1.00
1.00	0.99	0.98	0.98	0.98	0.97	0.98	0.97	0.97	0.97	1.10
1.00	0.99	0.99	0.98	0.98	0.98	0.98	0.98	0.98	0 98	1.20
1.01	1 00	0.99	0.99	0.99	0.99	0.99	0.99	0.98	0.98	1.30
1.01	1.00	1.00	0.99	0.99	0.99	0.99	0.99	0.99	0.99	1.40
1.01	1 00	1.00	1.00	1.00	0.99	1.00	1.00	0 99	0.99	1.50
1.02	1.01	1.01	1 00	1.00	1.00	1 00	1.00	1.00	1.00	1.60
1.02	1.01	1.01	1.01	1.00	1.00	1.00	1.00	1.00	1.00	1.70
1.02	1.01	1.01	1.01	1 01	1.01	1.01	1.01	1 01	1.01	1.80
1.02	1.02	1.02	1.01	1.01	1.01	1.01	1.01	1.01	1.01	1.90
1.03	1.02	1.02	1.01	1.01	1.01	1.01	1.01	1.01	1.01	2.00

TABLE VII.- VELOCITY RATIO

[Ratio of velocity for high-density rough case to velocity for low-density rough case (table V)]

D= 100	200	300	400	500	600	700	800	900	1000	Z/M
1.26	1.08	1.12	1.16	1.16	1.16	1.16	1.17	1.18	1.18	0.10
1.02	1.06	1.13	1.15	1.15	1.15	1.16	1.17	1.18	1.19	0.20
1.02	1.07	1.12	1.15	1.14	1.15	1.16	1.17	1.17	1.12	0.30
1.01	1.07	1.12	1.14	1.14	1.14	1.16	1.16	1.17	1.18	0.40
1.01	1.07	1.11	1.13	1.13	1.14	1.15	1.16	1.17	1.18	0.50
1.01	1.06	1.11	1.12	1.13	1.14	1.15	1.16	1.17	1.16	0.60
1.01	1.06	1.10	1.12	1.13	1.14	1.15	1.16	1.17	1.19	0.70
1.01	1.06	1.10	1.12	1.13	1.13	1.15	1.16	1.17	1.19	0.80
1.01	1.05	1.10	1.11	1.12	1.13	1.15	1.16	1.17	1.18	0.90
1.01	1.05	1.09	1.11	1.12	1.13	1.15	1.16	1.17	1.18	1.00
1.01	1.05	1.09	1.11	1.12	1.13	1.14	1.16	1.17	1.18	1.10
1.01	1.04	1.09	1.11	1.12	1.13	1.14	1.15	1.17	1.18	1.20
1.01	1.04	1.08	1.11	1.11	1.13	1.14	1.15	1.17	1.18	1.30
1.00	1.04	1.08	1.11	1.11	1.12	1.14	1.15	1.17	1.18	1.40
1.00	1.04	1.08	1.10	1.11	1.12	1.14	1.15	1.16	1.19	1.50
1.00	1.04	1.08	1.10	1.11	1.12	1.14	1.15	1.16	1.17	1.60
1.00	1.04	1.07	1.10	1.11	1.12	1.14	1.15	1.16	1.17	1.70
[illegible]										

TABLE VIII.- FLUX VALUES AT 0.8 METER

DIA MU M	P %	APEX SPEED M/S	SCALE HEIGHT M	EQUIV. MASS FLUX KG/M2-S	EQUIV CONC KG/M3	EQUIV. ENERGY FLUX J/M2-S	EQUIV. PARTICLE FLUX /M2-S	HITS PER DAY	PART. ENERGY MU J
100	8.00	34.9	0.006	3.3698E-54	9.666E-56	2.048E-51	2.429E-45	1.01E-46	1
200	17.00	26.8	0.013	2.7843E-27	1.040E-28	9.980E-25	2.508E-19	2.59E-20	4
300	44.00	19.9	0.019	7.5443E-18	3.798E-19	1.489E-15	2.014E-10	6.12E-11	7
400	13.00	15.3	0.026	3.1947E-13	2.085E-14	3.750E-11	3.598E-06	3.64E-07	10
500	5.00	11.9	0.034	2.0119E-10	1.686E-11	1.433E-08	1.160E-03	5.01E-05	12
600	4.00	9.6	0.041	1.3054E-08	1.360E-09	6.014E-07	4.355E-02	1.60E-03	14
700	3.00	7.9	0.049	2.1851E-07	2.757E-08	6.862E-06	4.591E-01	1.43E-02	15
800	3.00	6.7	0.057	2.0772E-06	3.132E-07	4.597E-05	2.924E+00	9.85E-02	16
900	2.00	5.7	0.066	1.1228E-05	1.968E-06	1.826E-04	1.110E+01	2.60E-01	16
1000	1.00	4.9	0.075	4.4026E-05	8.901E-06	5.386E-04	3.173E+01	4.11E-01	17

TOTAL MASS FLUX = 7.34E-07 KG/M2-S
TOTAL CONCENTRATION = 1.39E-07 KG/M3
TOTAL ENERGY FLUX = 1.06E-05 J M2-S
TOTAL HITS DAY OF SALTATION BY PARTICLES WITH K.E. >15 MU J = 7.78E-01
TOTAL EFFECTIVE HITS/DAY OF SALTATION = 8.83E-01
EXPECTED SENSOR LIFE = 1.46E+04 DAYS = 3.99E+01 YEARS

DIA	P	% MASS FLUX	% K.E. FLUX	% PARTICLE FLUX	% CONC	MASS FLUX KG M2S
100	8.00	0.00	0.00	0.00	0.00	2.696E-55
200	17.00	0.00	0.00	0.00	0.00	4.733E-28
300	44.00	0.00	0.00	0.00	0.00	3.320E-18
400	13.00	0.00	0.00	0.00	0.00	4.153E-14
500	5.00	0.00	0.01	0.01	0.00	1.006E-11
600	4.00	0.07	0.23	0.27	0.04	5.221E-10
700	3.00	0.89	1.93	2.14	0.60	6.555E-09
800	3.00	8.49	12.95	13.65	6.76	6.232E-08
900	2.00	30.58	34.30	34.55	28.40	2.246E-07
1000	1.00	59.96	50.58	49.38	64.21	4.403E-07

TABLE IX.- FLUX VALUES AT 1.2 METERS

DIA MU M	P %	AMBIENT WIND SPEED M/S	SCALE HEIGHT M	EQUIV. MASS FLUX KG/M2-S	EQUIV CONC KG/M3	EQUIV. ENERGY FLUX J/M2-S	EQUIV. PARTICLE FLUX #/M2-S	HITS PER DAY	PART. ENERGY MU J
100	8.00	38.2	0.007	8.3753E-71	2.191E-72	6.122E-68	6.036E-62	2.50E-63	1
200	17.00	30.8	0.014	2.4803E-36	8.055E-38	1.176E-33	2.234E-28	2.30E-29	5
300	44.00	23.9	0.021	3.5282E-24	1.478E-25	1.006E-21	9.418E-17	2.86E-17	11
400	13.00	18.8	0.029	5.7339E-18	3.048E-19	1.015E-15	6.457E-11	6.53E-12	16
500	5.00	15.0	0.037	2.7763E-14	1.846E-15	3.139E-12	1.601E-07	6.92E-09	20
600	4.00	12.2	0.045	8.3197E-12	6.802E-13	6.223E-10	2.776E 05	1.06E-06	22
700	3.00	10.2	0.053	4.0242E-10	3.948E-11	2.091E-08	8.455E-04	2.63E-05	25
800	3.00	8.6	0.062	8.4778E-09	9.809E-10	3.166E-07	1.193E-02	4.02E-04	27
900	2.00	7.5	0.071	8.8441E-08	1.187E-08	2.457E-06	8.743E-02	2.13E-03	28
1000	1.00	6.5	0.080	5.8410E-07	8.981E-08	1.235E-05	4.210E-01	5.46E-03	29

TOTAL MASS FLUX = 7.88E-09 KG/M2-S
TOTAL CONCENTRATION = 1.17E-09 KG/M3
TOTAL ENERGY FLUX = 1.83E-07 J M2-S
TOTAL HITS DAY OF SALTATION BY PARTICLES WITH K.E. >15 MU J = 8.00E-03
TOTAL EFFECTIVE HITS/DAY OF SALTATION = 2.32E-02
EXPECTED SENSOR LIFE = 5.54E+05 DAYS = 1.52E+03 YEARS

DIA	P	% MASS FLUX	% K.E. FLUX	% PARTICLE FLUX	% CONC	MASS FLUX IN HITS
100	8.00	0.00	0.00	0.00	0.00	6.700E-72
200	17.00	0.00	0.00	0.00	0.00	4.217E-37
300	44.00	0.00	0.00	0.00	0.00	1.552E-24
400	13.00	0.00	0.00	0.00	0.00	7.454E-19
500	5.00	0.00	0.00	0.00	0.00	1.383E-15
600	4.00	0.00	0.01	0.02	0.00	3.328E-13
700	3.00	0.15	0.34	0.40	0.10	1.207E-11
800	3.00	3.23	5.20	5.64	2.52	2.543E-10
900	2.00	22.46	26.87	27.57	20.35	1.769E-09
1000	1.00	74.16	67.57	66.37	77.02	5.841E-09

TABLE X.- FLUX VALUES AT 1.6 METERS

DIA MU M	P %	APEX SPEED M/S	SCALE HEIGHT M	EQUIV. MASS FLUX KG/M2-S	EQUIV CONC KG/M3	EQUIV. ENERGY FLUX J/M2-S	EQUIV. PARTICLE FLUX /M2-S	HITS PER DAY	PART. ENERGY MU J
100	8.00	40.5	0.008	7.5077E-85	1.852E-86	6.170E-82	5.411E-76	2.24E-77	1
200	17.00	33.7	0.016	3.4300E-44	1.016E-45	1.953E-41	3.090E-36	3.18E-37	6
300	44.00	26.9	0.023	9.8659E-30	3.673E-31	3.560E-27	2.633E-22	8.01E-23	14
400	13.00	21.6	0.031	3.3233E-22	1.541E-23	7.731E-20	3.742E-15	3.78E-16	21
500	5.00	17.5	0.040	1.1085E-17	6.347E-19	1.691E-15	6.391E-11	2.76E-12	26
600	4.00	14.4	0.048	1.1452E-14	7.960E-16	1.185E-12	3.821E-08	1.45E-09	31
700	3.00	12.1	0.057	1.3581E-12	1.122E-13	9.941E-11	2.854E-06	8.80E-08	35
800	3.00	10.3	0.066	5.9848E-11	5.802E-12	3.183E-09	8.424E-05	2.04E-06	38
900	2.00	8.9	0.075	1.1274E-09	1.263E-10	4.494E-08	1.115E-03	2.70E-05	40
1000	1.00	7.8	0.085	1.1579E-08	1.478E-09	3.553E-07	8.345E-03	1.0eE-04	13

TOTAL MASS FLUX = 1.40E-10 KG/M2-S
TOTAL CONCENTRATION = 1.75E-11 KG/M3
TOTAL ENERGY FLUX = 4.55E-09 J/M2-S
TOTAL HITS/DAY OF SALTATION BY PARTICLES WITH K.E. >15 MU J = 1.38E-04
TOTAL EFFECTIVE HITS/DAY OF SALTATION = 1.10E-03
EXPECTED SENSOR LIFE = 1.17E+07 DAYS = 3.19E+04 YEARS

DIA	P	% MASS FLUX	% K.E. FLUX	% PARTICLE FLUX	% CONC	MASS FLUX KG M2S
100	8.00	0.00	0.00	0.00	0.00	6.006E-86
200	17.00	0.00	0.00	0.00	0.00	5.831E-45
300	44.00	0.00	0.00	0.00	0.00	4.341E-30
400	13.00	0.00	0.00	0.00	0.00	4.320E-23
500	5.00	0.00	0.00	0.00	0.00	5.543E-19
600	4.00	0.00	0.00	0.00	0.00	4.581E-16
700	3.00	0.03	0.07	0.08	0.02	4.074E-14
800	3.00	1.28	2.10	2.33	1.00	1.795E-12
900	2.00	16.09	19.75	20.57	14.44	2.255E-11
1000	1.00	82.60	78.08	77.01	84.54	1.158E-10

TABLE XI.- SUMMARY OF FLUX VALUES AND SENSOR LIFETIMES

[Calculated for the rough high-density case (table V)]

MAP: SAND FLUXES
AIR DENSITY = 0.018 KG M3 L PRIME = 1 CM
V*PPIME = 3.53 M S LO = 300 MU M

TOTALS

Z*M	MASS FLUX	CONCENTRATION	F.E. FLUX	HITS/DAY	EFF. HITS DAY	LIFE-YRS
0.1	5.1E-02	3.1E-02	1.4E-01			
0.2	5.0E-03	2.1E-03	1.7E-02			
0.3	9.0E-04	2.7E-04	4.0E-03			
0.4	1.6E-04	4.6E-05	1.1E-03			
0.5	3.7E-05	9.3E-06	3.2E-04			
0.6	9.4E-06	2.1E-06	9.8E-05			
0.7	2.5E-06	5.2E-07	3.2E-05			
0.8	7.3E-07	1.4E-07	1.1E-05	7.8E-01	8.8E-01	40
0.9	2.2E-07	3.9E-08	3.7E-06	2.4E-01	3.3E-01	105
1.0	7.0E-08	1.2E-08	1.3E-06	7.2E-02	1.3E-01	268
1.1	2.3E-08	3.6E-09	4.9E-07	2.4E-02	5.4E-02	649
1.2	7.9E-09	1.2E-09	1.8E-07	8.0E-03	2.3E-02	[illegible]
1.3	2.8E-09	3.9E-10	7.0E-08	2.8E-03	1.0E-02	3409
1.4	1.0E-09	1.3E-10	2.9E-08	1.0E-03	4.3E-03	[illegible]
1.5	3.7E-10	4.7E-11	1.1E-08	3.6E-04	1.8E-03	[illegible]
1.6	1.4E-10	1.7E-11	4.5E-09	1.4E-04	1.1E-03	[illegible]
1.7	5.4E-11	6.5E-12	1.9E-09	5.3E-05	5.5E-04	[illegible]
1.8	2.1E-11	2.5E-12	8.0E-10	2.1E-05	2.3E-04	[illegible]
1.9	8.6E-12	9.7E-13	3.4E-10	7.3E-06	1.5E-04	[illegible]
2.0	3.5E-12	3.8E-13	1.5E-10	3.4E-06	7.8E-05	[illegible]

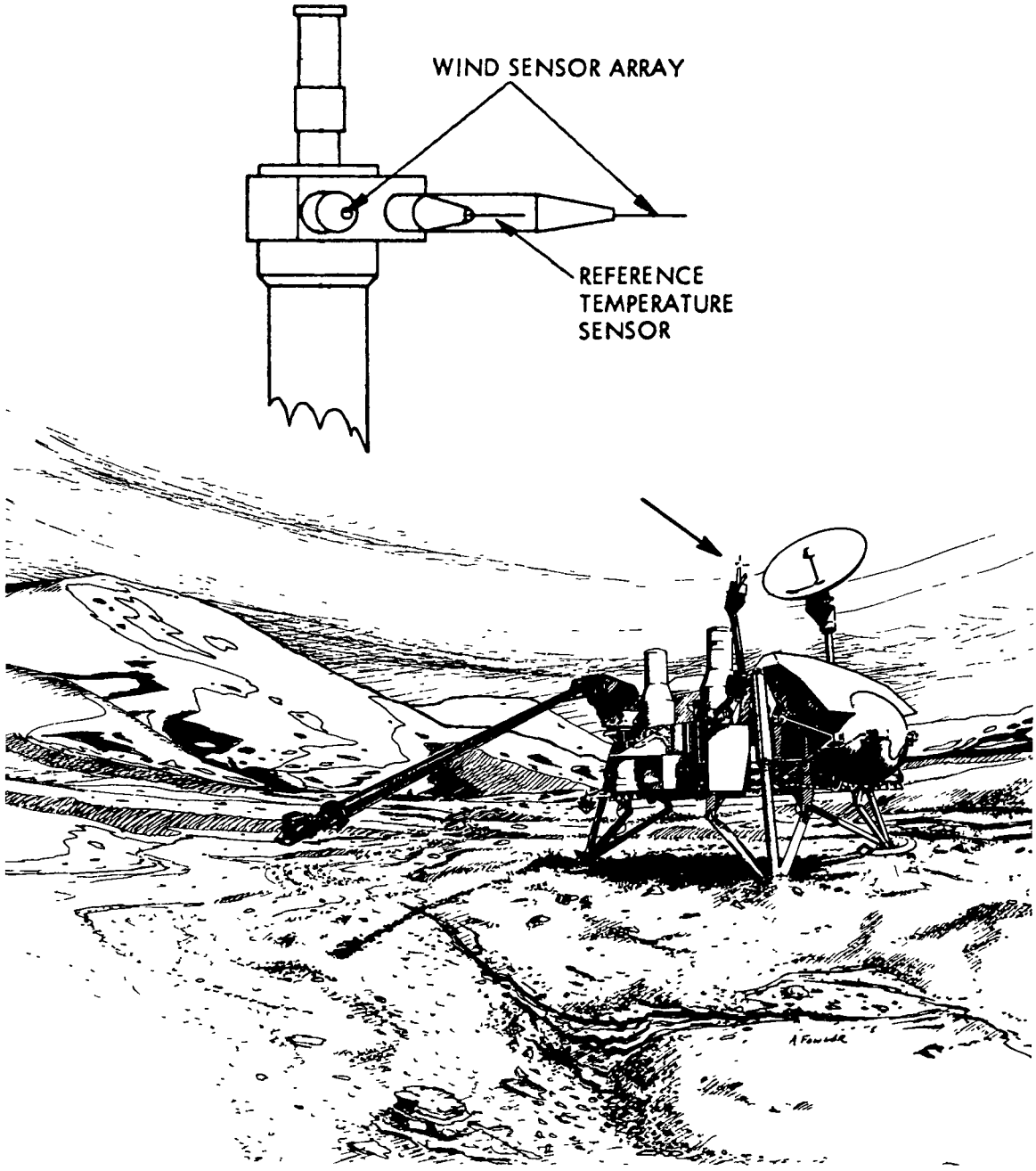

Figure 1.- Viking lander showing deployed position of wind sensors.

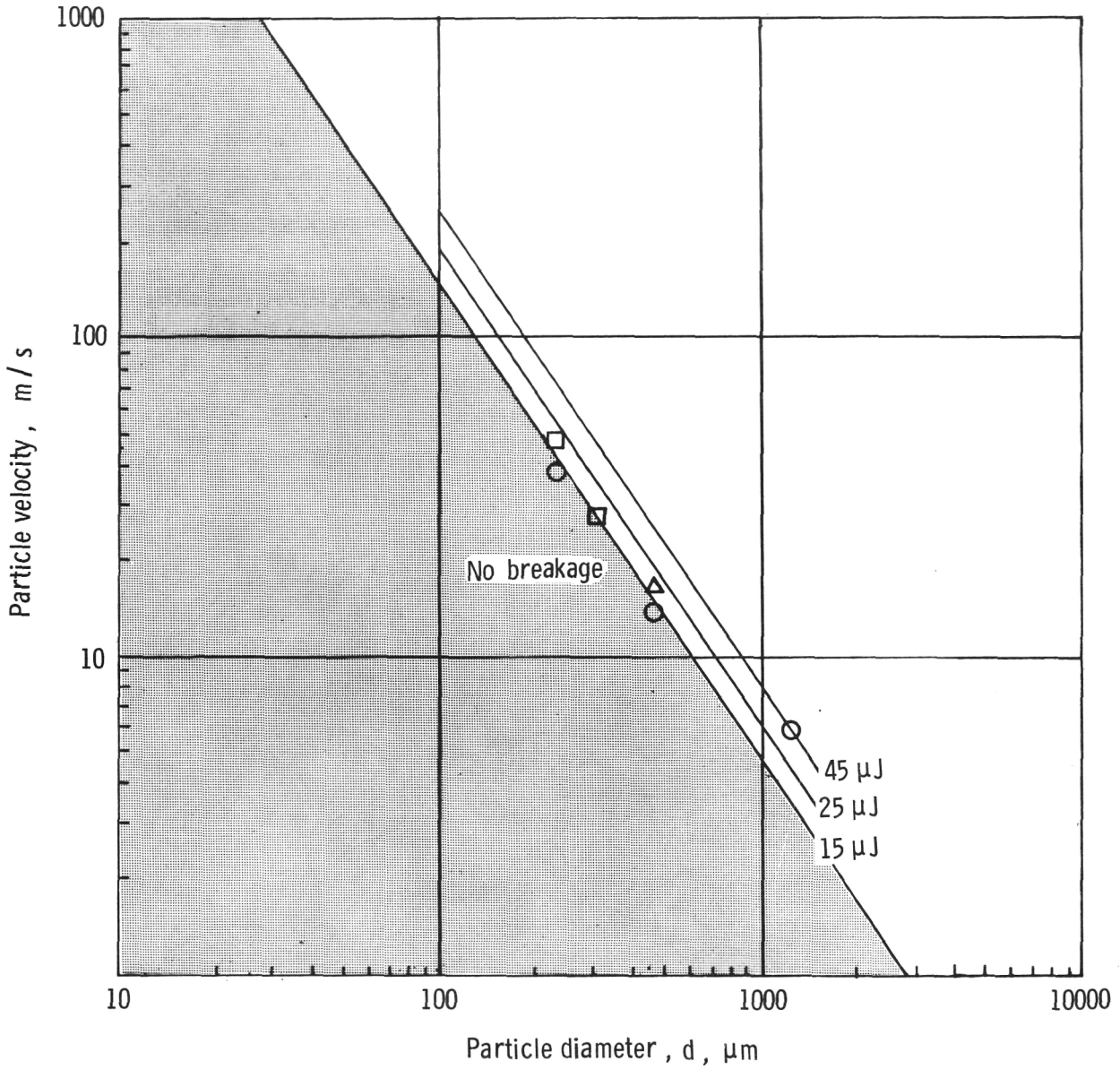

Figure 2.- Results of sensor-breakage tests. Symbols indicate particle velocity required to break the test subjects. Circles represent uncoated glass rods; squares represent prototype sensors; and the triangle, a flight-type sensor. Diagonal lines are constant values of kinetic energy.

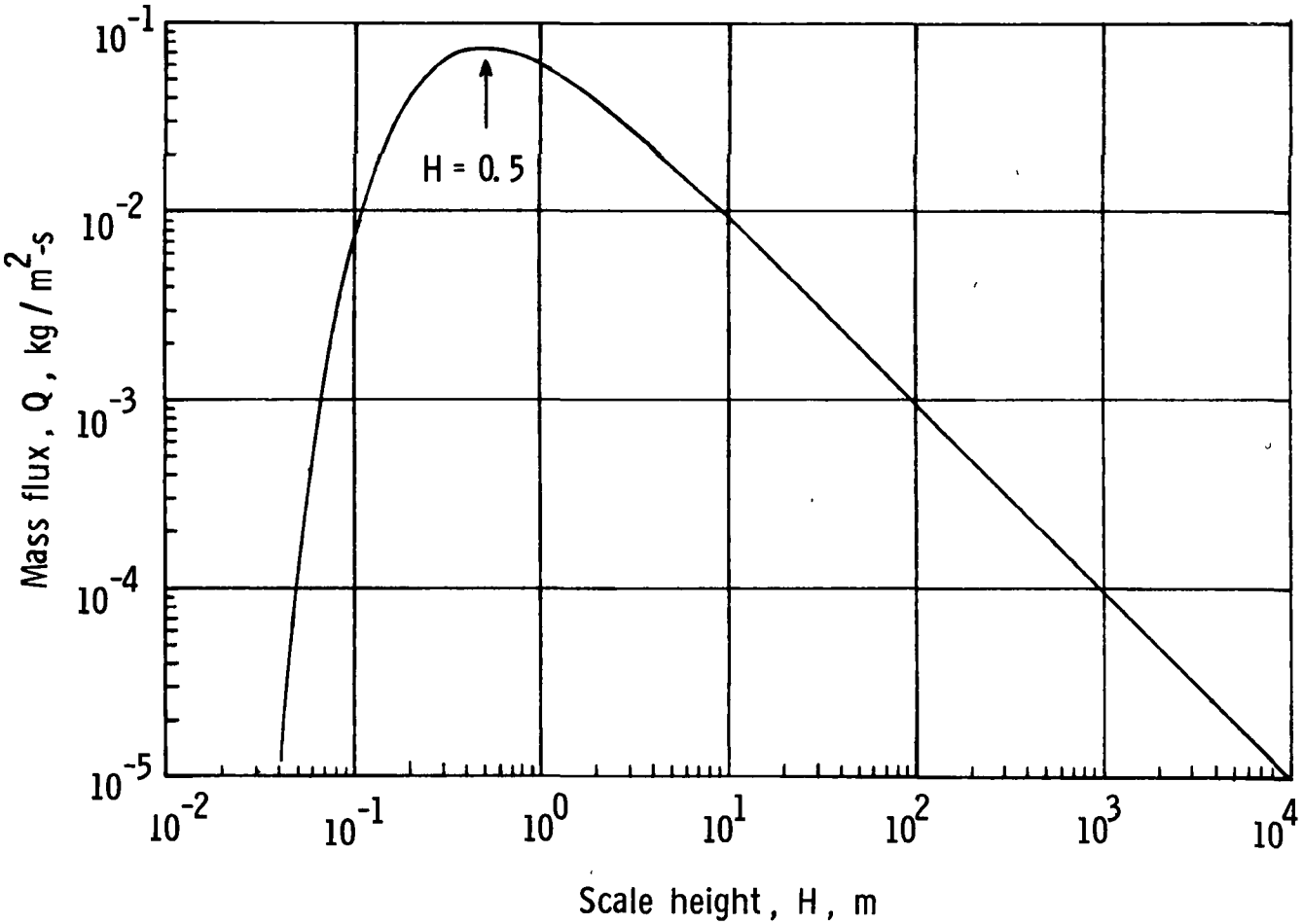

Figure 3.- Mass flux as a function of scale height for a constant elevation of 0.5 m.

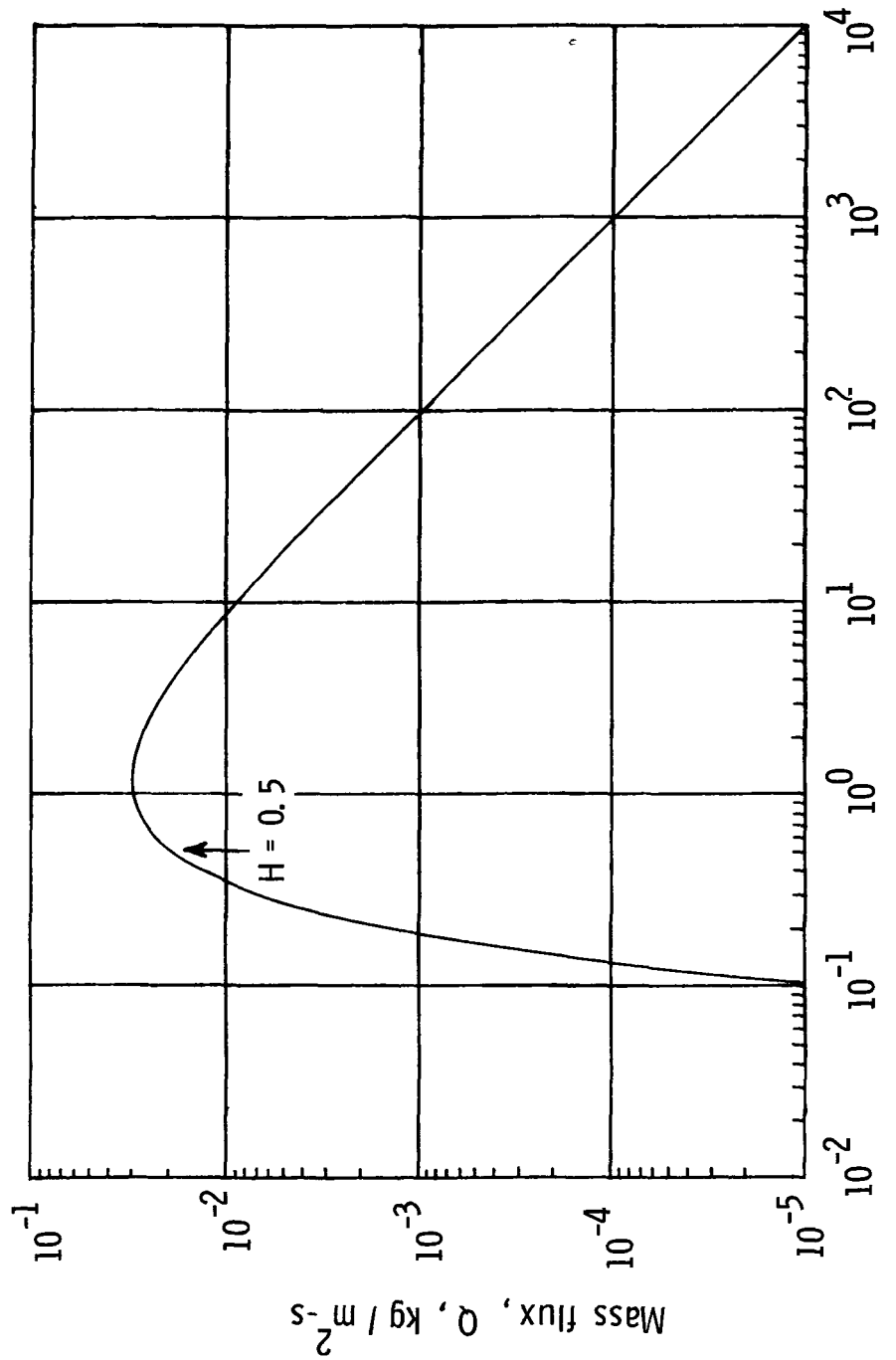

Figure 4.- Mass flux as a function of scale height at a constant elevation of 1.2 m.

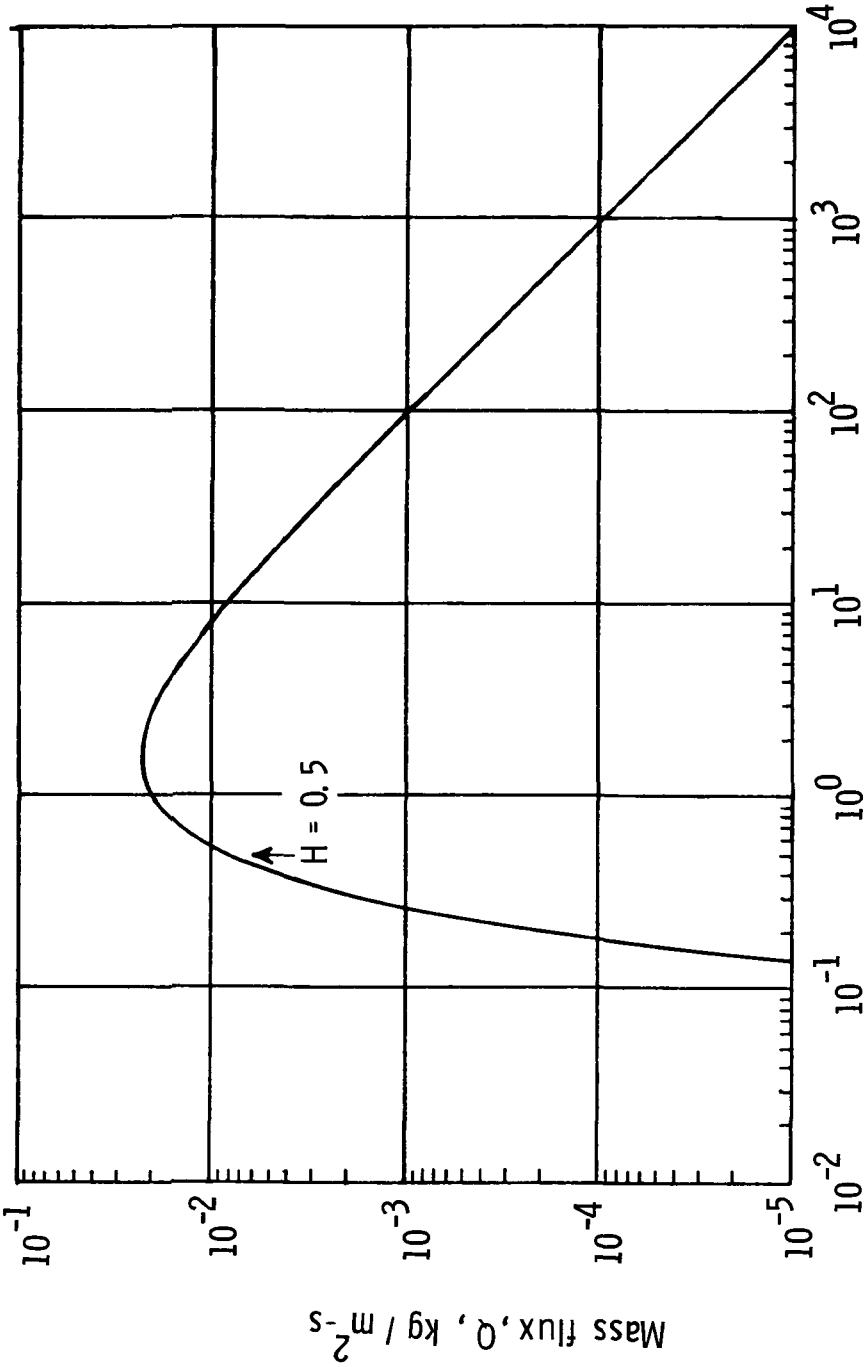

Figure 5.- Mass flux as a function of scale height at a constant elevation of 1.6 m.

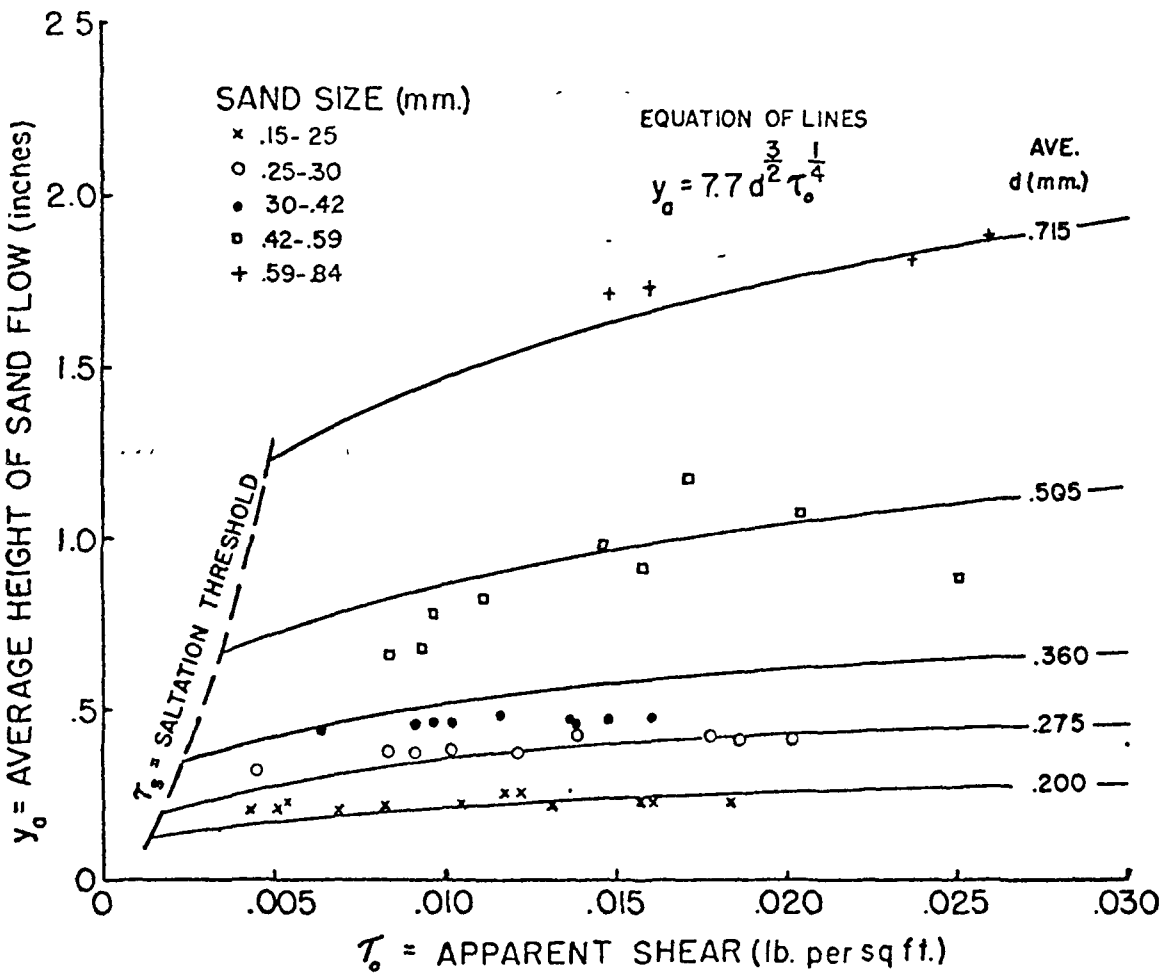

Figure 6.- Average height of saltation plotted against apparent shear $\left(\tau_O = \rho V_*^2\right)$ (from ref. 2).

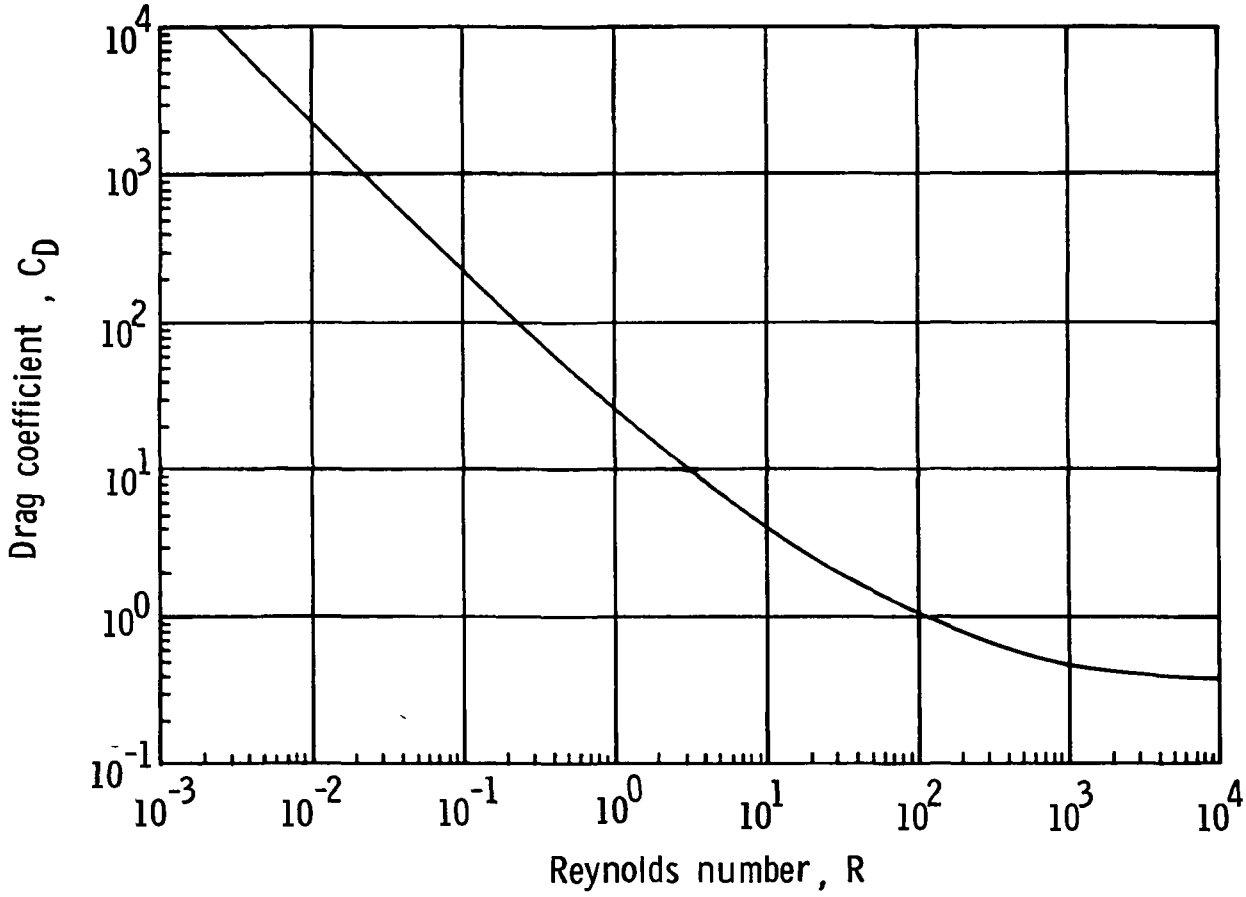

Figure 7.- Drag-coefficient function used in numerical trajectory simulations.

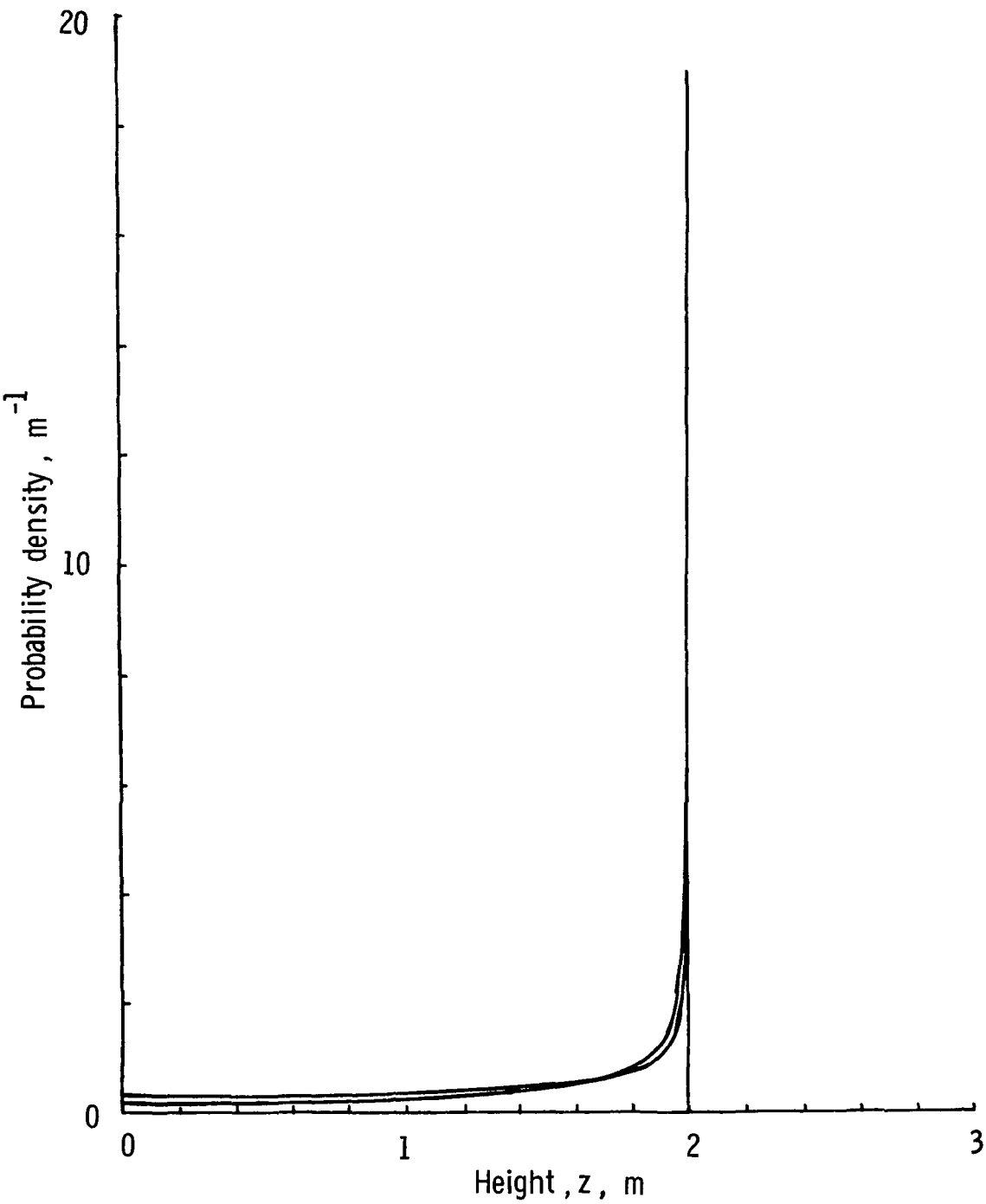

Figure 8.- Probability density per unit height for upward and downward portions of the trajectory of a 300-μm particle with an apex height of 2.0 m.

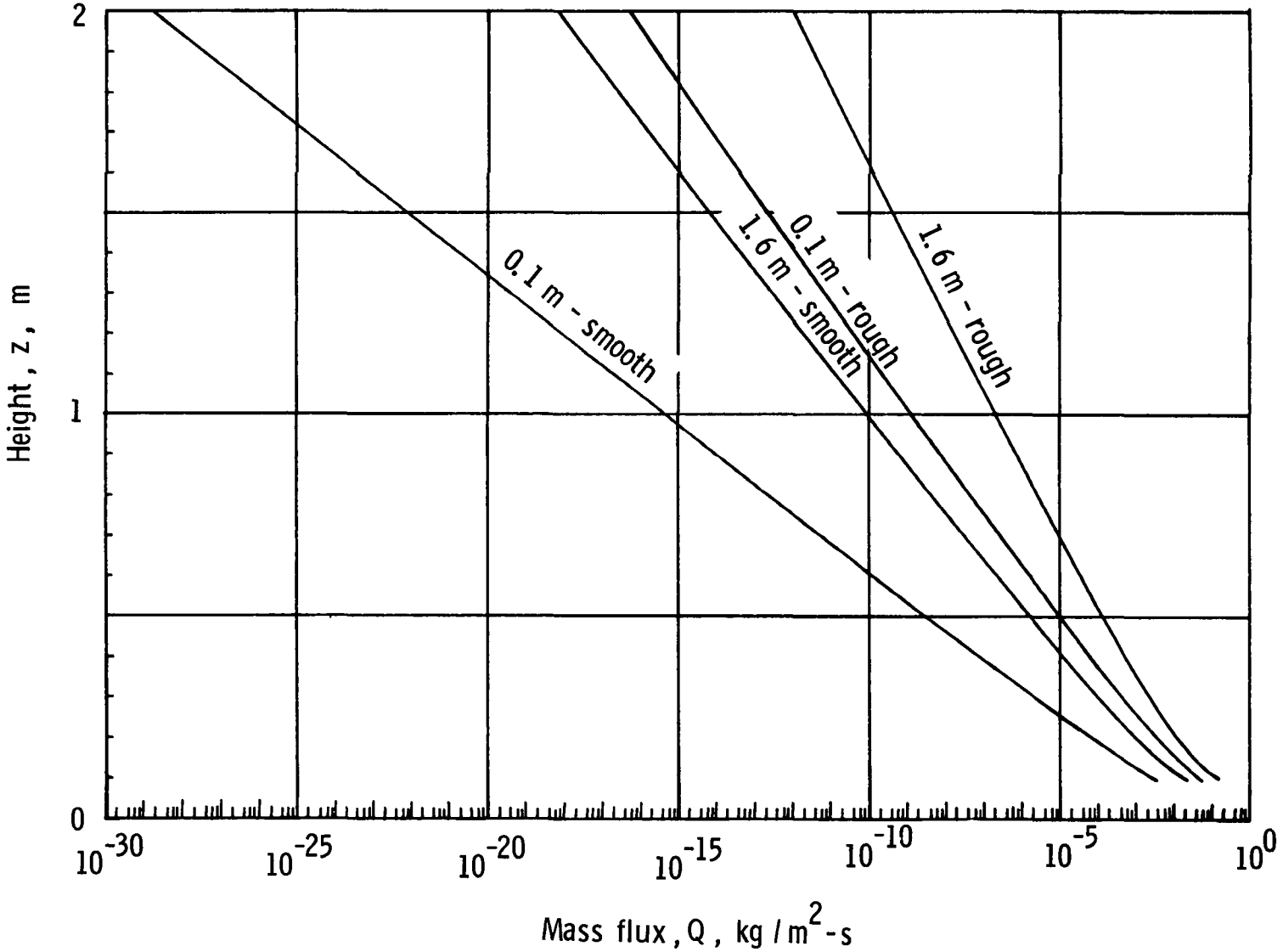

Figure 9.- Mass flux as a function of height for the high-density rough and smooth cases described in table V for scale heights based on Mars height of 0.1 m and 1.6 m.

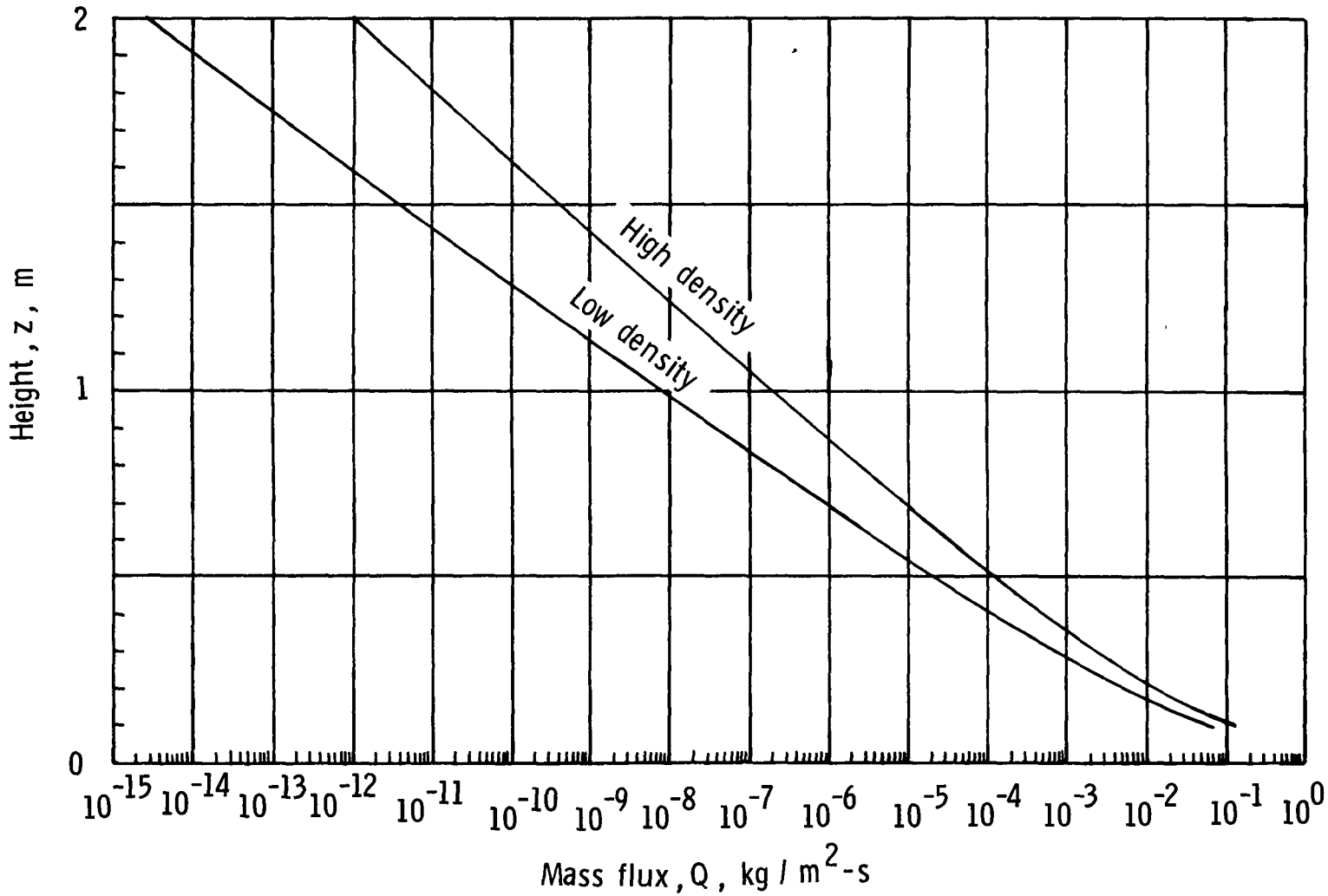

Figure 10.- Mass flux as a function of height for the high-density and low-density rough cases described in table V for scale heights based on Mars height of 1.6 m.

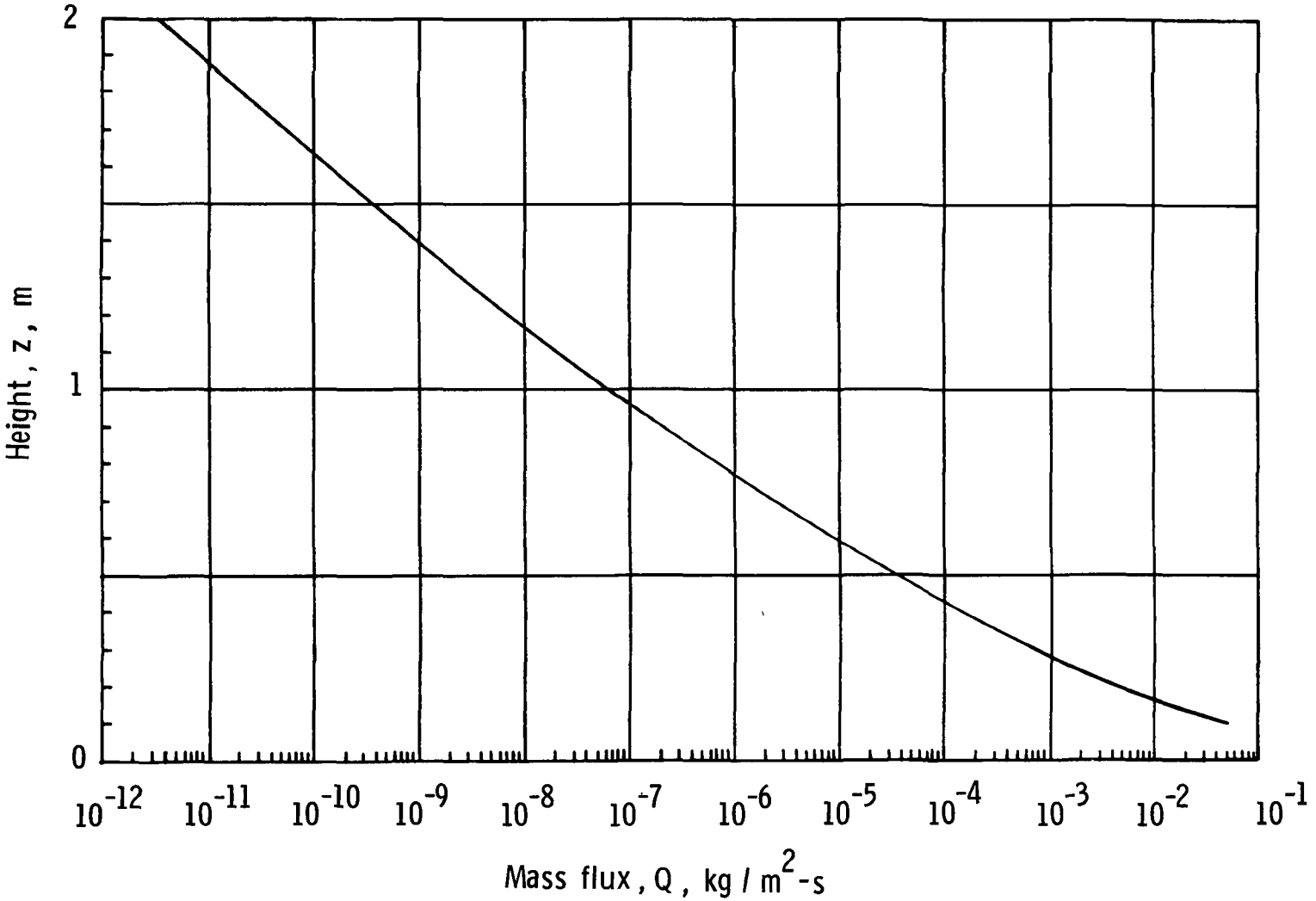

Figure 11.- Mass flux as a function of height for the high-density rough case described in table V for scale-height ratios computed individually for 0.1-m increment of Mars height.

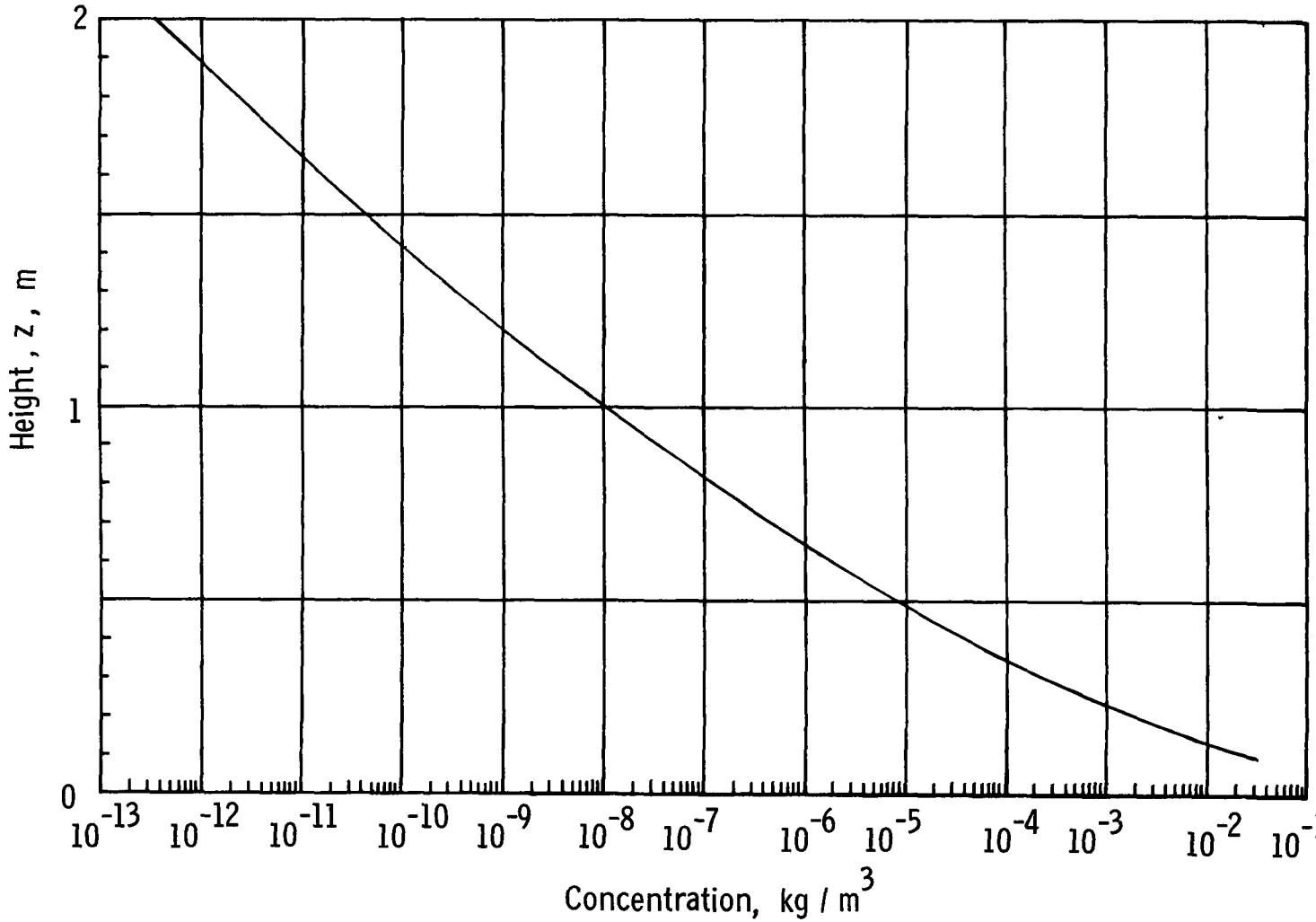

Figure 12.- Concentration as a function of height for the high-density rough case described in table V.

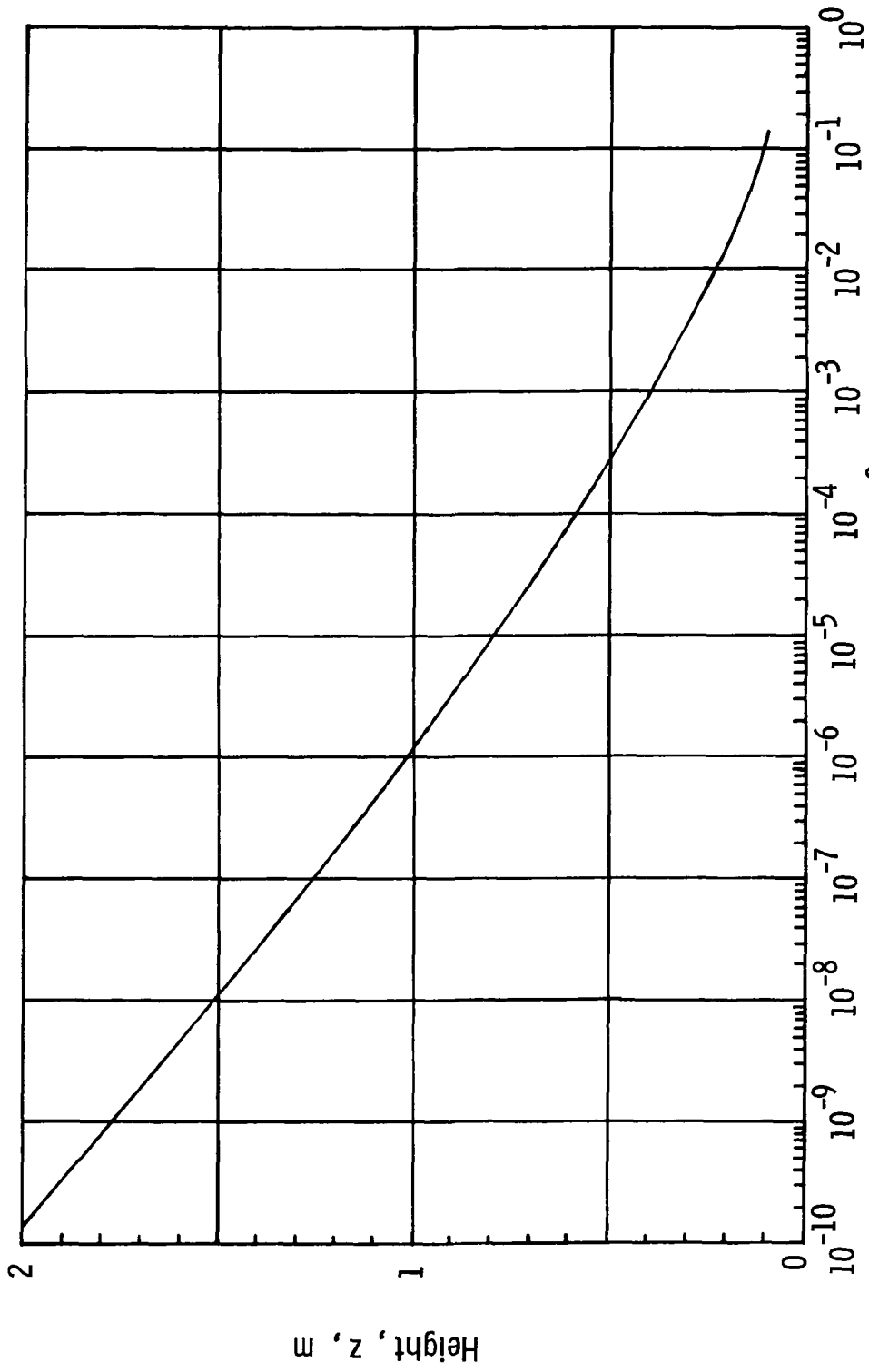

Figure 13.- Kinetic-energy flux as a function of height for the high-density rough case described in table V.

1 Report No	2 Government Accession No	3 Recipient's Catalog No
NASA TN D-8035		

4 Title and Subtitle	5 Report Date
SALTATION ON MARS AND EXPECTED LIFETIME OF VIKING 75 WIND SENSORS	December 1975
	6 Performing Organization Code
7 Author(s)	8 Performing Organization Report No
Robert M. Henry	L-9871
	10 Work Unit No
9 Performing Organization Name and Address	815-20-04-06
NASA Langley Research Center Hampton, Va. 23365	11 Contract or Grant No
	13 Type of Report and Period Covered
12 Sponsoring Agency Name and Address	Technical Note
National Aeronautics and Space Administration Washington, D.C. 20546	14 Sponsoring Agency Code

15 Supplementary Notes

16 Abstract

With the use of the wind-tunnel measurements of Bagnold and Zingg, a model is developed for estimating the parameters that describe the flux of sand on Mars. Application of this model to the sensor-breakage problem indicates that the expected lifetime on Mars of the wind sensors of the Viking 75 Meteorology Instrument System is about 40 Earth years. This expected lifetime is adequate for both the primary Viking 75 mission and for a proposed extended mission.

17 Key Words (Suggested by Author(s))	18 Distribution Statement
Anemometers Saltation Mars Viking Sand	Unclassified – Unlimited Subject Category 91

19 Security Classif (of this report)	20 Security Classif (of this page)	21 No of Pages	22 Price*
Unclassified	Unclassified	39	$3.75

*For sale by the National Technical Information Service, Springfield, Virginia 22161

"The aeronautical and space activities of the United States shall be conducted so as to contribute . . to the expansion of human knowledge of phenomena in the atmosphere and space The Administration shall provide for the widest practicable and appropriate dissemination of information concerning its activities and the results thereof"

—NATIONAL AERONAUTICS AND SPACE ACT OF 1958

NASA SCIENTIFIC AND TECHNICAL PUBLICATIONS

TECHNICAL REPORTS Scientific and technical information considered important, complete, and a lasting contribution to existing knowledge

TECHNICAL NOTES Information less broad in scope but nevertheless of importance as a contribution to existing knowledge

TECHNICAL MEMORANDUMS Information receiving limited distribution because of preliminary data, security classification, or other reasons Also includes conference proceedings with either limited or unlimited distribution.

CONTRACTOR REPORTS Scientific and technical information generated under a NASA contract or grant and considered an important contribution to existing knowledge

TECHNICAL TRANSLATIONS Information published in a foreign language considered to merit NASA distribution in English

SPECIAL PUBLICATIONS Information derived from or of value to NASA activities. Publications include final reports of major projects, monographs, data compilations, handbooks, sourcebooks, and special bibliographies

TECHNOLOGY UTILIZATION PUBLICATIONS Information on technology used by NASA that may be of particular interest in commercial and other non-aerospace applications Publications include Tech Briefs, Technology Utilization Reports and Technology Surveys

Details on the availability of these publications may be obtained from:

SCIENTIFIC AND TECHNICAL INFORMATION OFFICE

NATIONAL AERONAUTICS AND SPACE ADMINISTRATION

Washington, D.C. 20546